UNIVERSITÀDELLACALABRIA

Dipartimento di INFORMATICA , MODELLISTICA , ELETTRONICA e SISTEMISTICA

Master In Robotics and Automation

Active Rear Wheel Steering and Direct Yaw Moment Control

Finale Project of Vehicle Control Mod_1

Professor:

Prof. Alessandro Casavola

Prof. Gianfranco Gagliardi

Student:

Alexis Marino-Salguero

(232601)

Academic year 2021/2022

Table of Contents

1. Introduction

1.1. Four wheels steering system.

Four-wheel steering is a mechanism in cars, trucks, and trailers that allow all four wheels to turn in response to the driver's commands. This system is different with respect to line production vehicles which base their steering only on the front wheels while the rear wheels are fixed and follow the direction of the front wheels helped by a differential. four-wheels steering systems can make the driving experience more responsive and it can help drivers to turn and manoeuvre faster.

Four-wheel steering Improves maneuverability, it allows the rear wheels to turn in the opposite direction to the front wheels at low speeds, reducing the turning radius and enhancing maneuverability. This feature is especially beneficial in tight spaces, parking, and navigating narrow roads.

At higher speeds, the system can turn the rear wheels in the same direction as the front wheels, improving stability during lane changes, cornering, and high-speed maneuvers. This coordinated movement increases the vehicle's responsiveness and reduces the risk of oversteer or understeer. The added maneuverability and stability help drivers maintain control over the vehicle, potentially reducing the risk of accidents.

With four-wheel steering, vehicles exhibit improved agility and responsiveness. The rear wheels can assist with steering inputs, leading to quicker and more precise handling. This technology enhances the overall driving experience, especially in sporty or performance-oriented vehicles.

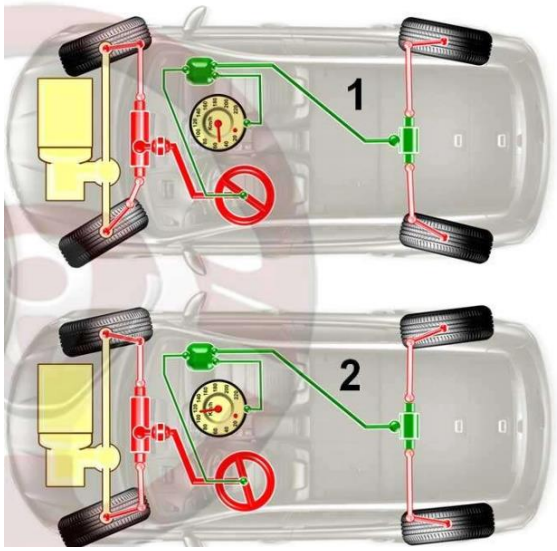

Fig1. Four wheels steering vehicle.

A general overview of how a four-wheel steering system works:

When the driver turns the steering wheel, a sensor or position sensor detects the input and sends a signal to the control unit of the 4WS system. The control unit receives the steering input signal and processes it along with other sensor inputs such as vehicle speed, wheel speed, and yaw rate. It calculates the appropriate steering angles for the front and rear wheels based on the driving conditions.

The control unit determines the desired angle for the front wheels based on the steering input and the driving conditions. It sends signals to the front wheel steering system (usually a conventional rack-and-pinion system) to turn the front wheels accordingly.

There are two main types of rear wheel steering systems:

Mechanical System: In some older or simpler 4WS systems, mechanical linkages are used to connect the front and rear wheels. And Electronic System: Modern 4WS systems often use electronic actuators to control the rear wheel steering.

The control unit continuously monitors the vehicle's speed, lateral acceleration, and other parameters to determine the optimal steering angles for both the front and rear wheels. At low speeds, the rear wheels can turn in the opposite direction to the front wheels, reducing the turning radius and improving maneuverability. At higher speeds, the rear wheels may turn in the same direction as the front wheels to enhance stability during lane changes and cornering as show the fig.2.

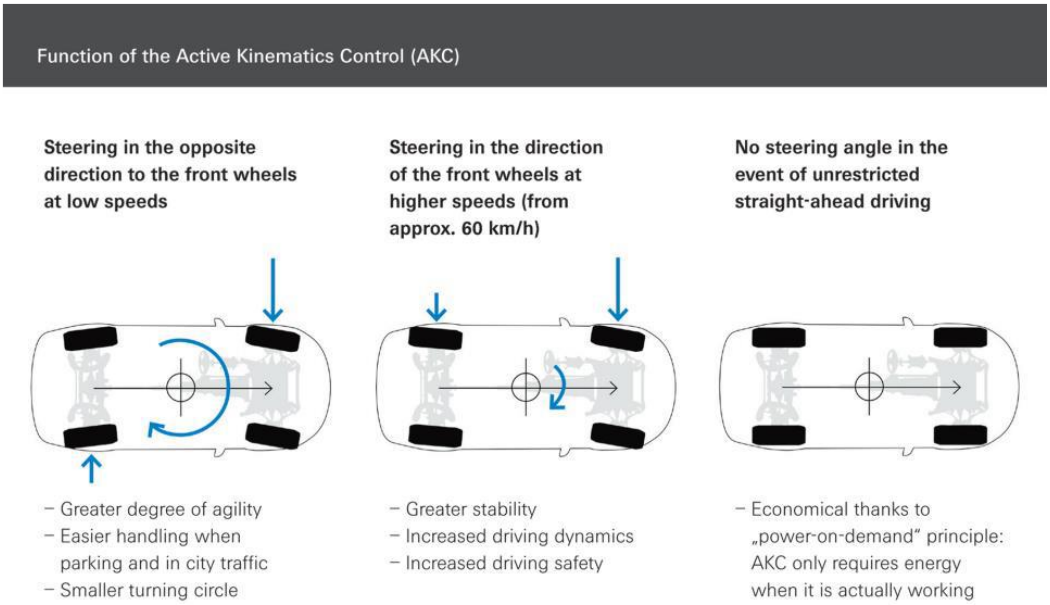

Fig.2 Function of the active kinematic control

1.2. Direct Yaw Moment

Direct yaw moment refers to the rotational motion around the vertical axis (yaw) of a vehicle, this situation can occur due to cornering at high speed, or due to poor road surface conditions. This is closely related to oversteering and understeering situations in vehicles.

Oversteer occurs when the rear wheel of the vehicle loses traction and begins to slide outwards during a turn, resulting in excessive yaw motion, while understeer happens when the front wheels lose traction and fail to turn as much as intended, causing the vehicle to continue moving in a straighter path rather than following the desired steering input.

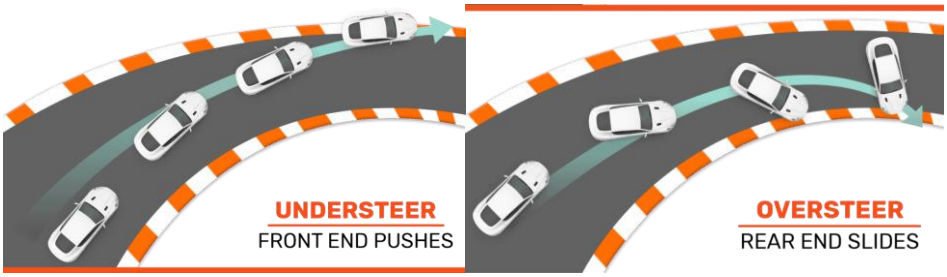

Fig.3 Understeer and oversteer situations.

Four-wheel steering systems (4WS) have been researched and developed along the time to improve handling and stability characteristics. Especially various active control systems for rear wheel steering have been developed by feed forward and/or feedback compensations for side slip motion in vehicle body. Although the improvement of handling and stability results in quite a good effect on driver steering manoeuvres, so-called, a closed loop performance of driver-

vehicle system, it is limited within a linear dynamical system because of the decrease of cornering stiffness of tires during a high lateral acceleration.

Direct yaw moment control systems (DYC) using driving/braking forces have been researched and developed also to improve handling and stability. One of them is active traction control system of each wheel through the feedback of state variables, such as yaw rate. The other is active braking control system through the feedback of state variables, such as yaw rate and/or side slip angle in vehicle body. These active control systems can generate yaw moment directly to compensate for vehicle yaw motion not only in linear ranges but also in nonlinear ranges of tire performance.

In situations where the vehicle is experiencing oversteer, direct yaw moment control with active rear steering can intervene by applying brake force selectively and turning the rear wheels in the opposite direction to the front wheels. This combination generates a direct yaw moment that helps to stabilize the vehicle and bring the rear end back in line with the desired trajectory. In understeer situations, direct yaw moment control with active rear steering can assist by applying brake force selectively and turning the rear wheels in the same direction as the front wheels. This coordinated movement generates a direct yaw moment that aids in enhancing the vehicle's steering response and improving cornering capability.

Report structure

In this project, an integrated control system design for active rear wheel steering and direct yaw moment control is presented. The proposed control system is a model matching controller (MMC) which makes the vehicle follow the desired dynamic model by using the state feedback of both yaw rate and side slip angle. Although this integrated MMC is designed by linear control theory, it can greatly improve the handling and the stability and show the expected robustness when the vehicle parameter change, such as, the vehicle mass, even in large lateral acceleration ranges. The steps to take are:

- Obtain the Model Matching Controller and implement in the Simulink environment.
- Develop the Feedback state controller using optimal control techniques.
- Comparison of optimal control techniques.
- Integrate an integral effect to the model and implement optimal controllers.
- Finally, varying the velocity to observe the robustness of the system and implement a gain scheduling control.

2. Modelling

2.1. Non-linear system model

Four-wheel steering systems have been researched based on the two-degree-of-freedom (2DOF) steering model shown in fig. 4. Systems equations of this model governing the side slip angle and the yaw rate are developed as follows.

Nomenclature

$\boldsymbol{\beta}$	Side slip angle of the vehicle body
$\boldsymbol{\gamma}$	Yaw rate of the vehicle body
$\boldsymbol{\delta_{sw}}$	Steering wheel angle
$\boldsymbol{\delta_f}$	Front wheel steering angle input
$\boldsymbol{\delta_r}$	Rear wheel steering angle input
$\boldsymbol{N}$	Direct yaw moment input
$\boldsymbol{V}$	Vehicle velocity
$\boldsymbol{m}$	Vehicle mass
$\boldsymbol{I_z}$	Yaw moment of inertia
$\boldsymbol{a_f, a_r}$	Distance from the center of gravity to front/rear axle
$\boldsymbol{c_f, c_r}$	Cornering stiffness at front/rear tire
$\boldsymbol{\alpha_f, \alpha_r}$	Slip angle at front/real wheels

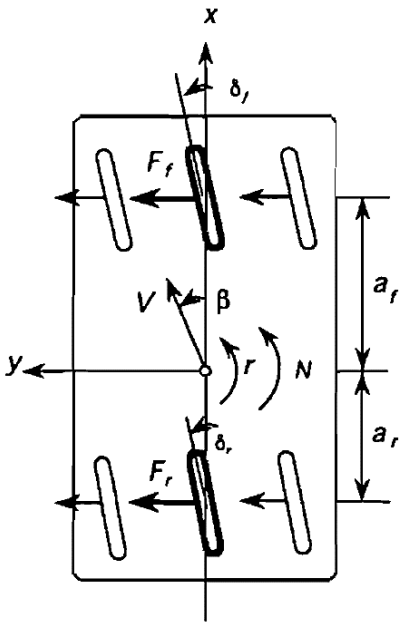

Fig.4. 2-DOF vehicle model

As we can see in Fig. 4, the vehicle has cornering ability based on the front and rear steering angles of the wheels. For small tire slip angles, the lateral tire forces can be approximated as a linear functions of tire slip angle. The front and rear tire forces and tire slip angles are defined as follows:

$$F_{yf} = C_f \alpha_f \quad (1)$$

$$F_{yr} = C_r \alpha_r \quad (2)$$

The longitudinal forces on the wheels are:

$$F_x = -F_{tf}(a_f)\sin(\delta_f) - F_{tr}(a_r)sin(\delta_r) \quad (3)$$

The rotational forces are:

$$M_{zf} = F_{yf} * a_f \quad (4)$$

$$M_{zr} = F_{yr} * a_r \quad (5)$$

The system of equations that identifies the dynamics of the vehicle is found with the application of Newton's principles.

Lateral Dynamics:

$$ma_y = \sum F_y = F_f + F_r = C_f \alpha_f + C_r \alpha_r \quad (6)$$

The lateral acceleration can be obtained with the following equation:

$$a_y = \dot{V}\sin(\beta) + Vcos(\beta)\dot{\beta} + V\gamma\cos(\beta) \quad (7)$$

Rotational Dynamic

$$I_z\dot{\gamma} = \sum M_Z = F_{yf} * a_f + F_{yr} * a_r \quad (8)$$

The front and rear slip angles are:

$$\alpha_f = \delta_f - \beta_f \quad (9)$$

$$\alpha_r = \delta_r - \beta_r \quad (10)$$

The angles can be obtained as follows:

Longitudinal component:

$$V_r \cos(\beta_r) = V cos(\beta) = V_f \cos(\beta_f) \quad (11)$$

Lateral component:

$$V_r \sin(\beta_r) = V \sin(\beta) - a_r \gamma \quad (12)$$

$$V_f \sin(\beta_f) = V \sin(\beta) - a_f \gamma \quad (13)$$

Now divide all for $cos(\beta_r, \beta_f)$

$$\tan(\beta_r) = \tan(\beta) - \frac{a_r \gamma}{V cos(\beta)} \quad (14)$$

$$\tan(\beta_f) = \tan(\beta) + \frac{a_f \gamma}{V cos(\beta)} \quad (15)$$

The equation that describes the non-linear system are:

$$m\dot{V} \sin(\beta) + mV cos(\gamma + \dot{\beta}) = C_f(\delta_f - \beta_f) + C_r(\delta_r - \beta_r) \quad (16)$$

$$I_z \dot{\gamma} = C_f a_f(\delta_f - \beta_f) + C_r a_r(\delta_r - \beta_r) \quad (17)$$

2.2. Linearization

The linearization of the system is developed with the following assumptions:

- Small variation of the angle β_f, β_f, β
- No longitudinal acceleration

With these conditions the equations 14, 15. 16 and 17 become in the following simplifications:

$$\beta \approx 0 \rightarrow \cos(\beta) = 1; \quad \sin(\beta) = \beta; \quad \tan(\beta) = \beta$$

$$\beta_f = \beta + \frac{a_f \gamma}{V} \quad (18)$$

$$\beta_r = \beta - \frac{a_r \gamma}{V} \quad (19)$$

The linear equations of the system are:

$$mV(\gamma + \dot{\beta}) = C_f(\delta_f - \beta - \frac{a_f \gamma}{V}) + C_r(\delta_r - \beta + \frac{a_r \gamma}{V}) \quad (20)$$

$$I_z \dot{\gamma} = C_f a_f \left(\delta_f - \beta - \frac{a_f \gamma}{V}\right) + C_r a_r \left(\delta_r - \beta + \frac{a_r \gamma}{V}\right) + \mathrm{N} \quad (21)$$

The equations of the 2DOF motions can be written in the following state space from.

$$\dot{x} = Ax + Bu + E\delta_f \quad (22)$$

Where, the front steering angle is considered a disturbance. the state vector including the side slip angle and the yaw rate and the input vector including the rear steer and the direct yaw moment are written as follows:

$$x = \begin{bmatrix} \beta \\ \gamma \end{bmatrix}, \qquad u = \begin{bmatrix} \delta_r \\ N \end{bmatrix} \quad (23)$$

And the coefficient matrices are:

$$A = \begin{bmatrix} -\frac{C_f+C_r}{mV} & -\frac{a_f C_f - a_r C_r}{mV^2} - 1 \\ -\frac{a_f C_f - a_r C_r}{I_z} & -\frac{{a_f}^2 C_f - {a_r}^2 C_r}{I_z V} \end{bmatrix} \quad (24)$$

$$B = \begin{bmatrix} \frac{C_r}{mV} & 0 \\ -\frac{a_r C_r}{I_z} & \frac{1}{I_z} \end{bmatrix},\ E = \begin{bmatrix} \frac{C_f}{mV} \\ \frac{a_f C_f}{I_z} \end{bmatrix},$$

2.3. Model design

Reference model

Because we have two control inputs in this two-degree-of-freedom system, any dynamical performance can be realized by state feedback compensation. Therefore, two independent first-order systems can be made as desired dynamical performances for each motion of the yaw rate and the side slip angle. This desired response model can be described by the transfer function.

$$x_d = \begin{bmatrix} \beta_d \\ \gamma_d \end{bmatrix} = \begin{bmatrix} \frac{k_\beta}{1+\tau_\beta s} \\ \frac{k_\gamma}{1+\tau_\gamma s} \end{bmatrix} \delta_f \quad (25)$$

And it is written in a state space form as follows.

$$\dot{x}_d = A_d x_d + E_d \delta_f \quad (26)$$

Where the coefficient matrices are

$$A_d = \begin{bmatrix} -\frac{1}{\tau_\beta} & 0 \\ 0 & -\frac{1}{\tau_\beta} \end{bmatrix},\quad E = \begin{bmatrix} \frac{k_\beta}{\tau_\beta} \\ \frac{k_\gamma}{\tau_\gamma} \end{bmatrix} \quad (27)$$

The parameters of the desired model can be chosen randomically, but these must be chosen in such a way as to reduce unrealistic control inputs.

Tracking error

In order to make the outputs of the actual vehicle follows the outputs of the desired model, the error variables are defined.

$$e = x - x_d = \begin{bmatrix} \Delta\beta \\ \Delta\gamma \end{bmatrix} \quad (28)$$

The equation concerning the error function is derived from the equation 22 and 26.

$$\begin{aligned} \dot{e} = \dot{x} - \dot{x}_d &= \left(Ax + Bu + E\delta_f\right) - \left(A_d x_d + E_d \delta_f\right) \\ &= A(x - x_d) + Bu + (A - A_d)x_d + (E - E_d)\delta_f \end{aligned} \quad (29)$$

Here, if the following is defined.

$$Bu_{fb} = Bu + (A - A_d)x_d + (E - E_d)\delta_f \quad (30)$$

Then the equation governing the error variables are obtained as follows.

$$\dot{e} = Ae + Bu_{fb} \quad (31)$$

This equation means that the stability of the error can be compensated by the state feedback controller, becoming in a zero-regulation problem.

States feedback gain

The error model can be compensated by an input controller (state feedback controller) as follows.

$$u_{fb} = -Fe \tag{32}$$

The elements of the matrix are.

$$\begin{bmatrix}\delta_f \\ N\end{bmatrix} = -\begin{bmatrix}F_{11} & F_{12} \\ F_{21} & F_{22}\end{bmatrix}\begin{bmatrix}\Delta\beta \\ \Delta\gamma\end{bmatrix} \tag{33}$$

Feed forward gain

The overall control inputs to the actual vehicle system Eq.22 are the summation of the feed forward and feedback compensation as follows.

$$u = u_d + u_{fb} \tag{34}$$

Or

$$\begin{bmatrix}\delta_f \\ N\end{bmatrix} = \begin{bmatrix}\delta_{rd} \\ N_d\end{bmatrix} + \begin{bmatrix}\Delta\delta_f \\ \Delta N\end{bmatrix} \tag{35}$$

Where the feed forward controller input is obtained from the equations 30 and 34.

$$u_d = -B^{-1}(A - A_d)x_d - B^{-1}(E - E_d)\delta_f \tag{36}$$

This feed forward controller can be transformed to the following by using equation 26.

$$u_d = -B^{-1}[(A - A_d)(sI - A_d)^{-1}E_d + (E - E_d)]\delta_f \tag{37}$$

Where s denotes a Laplace operator. The matrices of this equation are all given by equations 24 and 27.

Model matching controller.

This model matching control system is shown in the block diagram of Fig.5 and Fig.6. The gain matrix of the feedback controller F in equation 32 can be obtained to minimize the error by using optimal control theory with LMI tool.

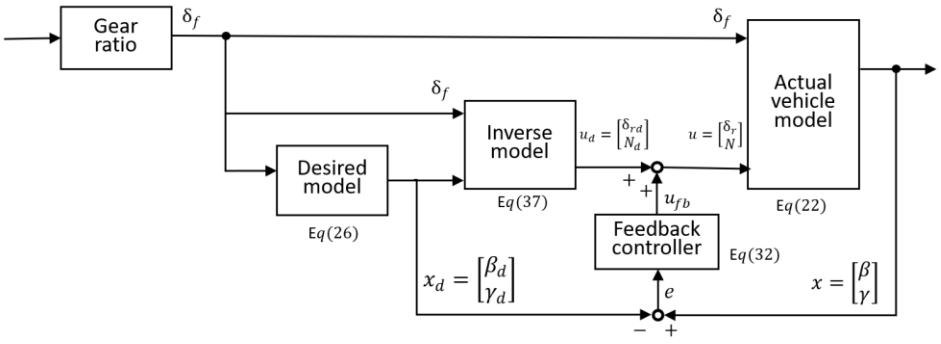

Fig.5. Block diagram of the Model Matching Controller

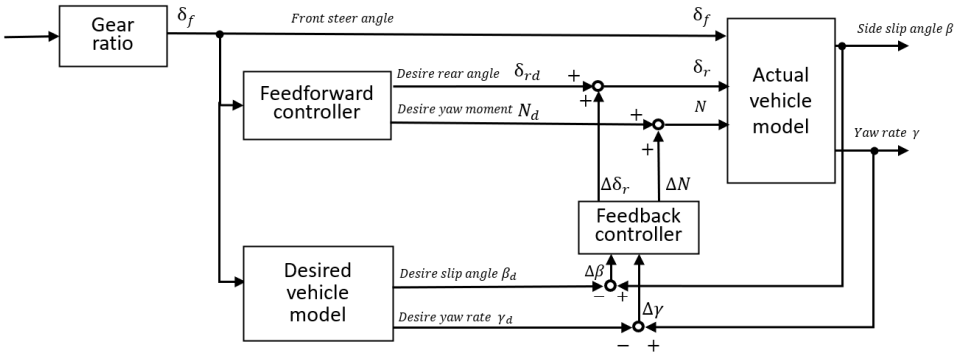

Fig.6. Equivalent block diagram of the Model Matching Controller

Modelling in MATLAB/Simulink environment

To carry out the simulation, a Simulink diagram was designed, which can reproduce the Model matching controller.

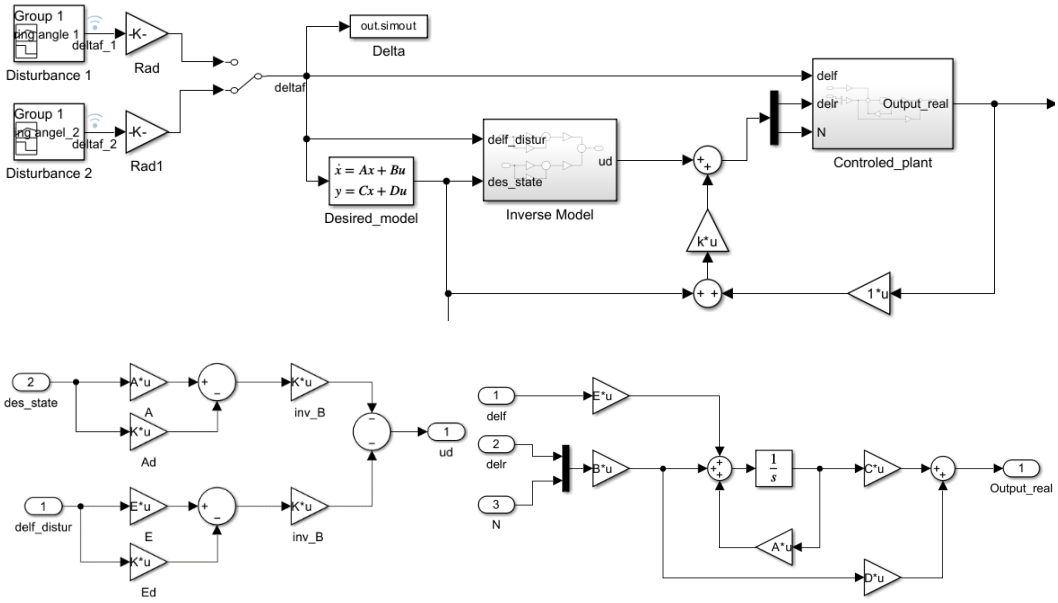

Fig.7. Simulink diagram of the Model Matching Controller

Disturbance signals

Remember that the front steering angle corresponds to a disturbance signal. Two different signals were considered as system disturbances as show the Fig.8 and Fig.9.

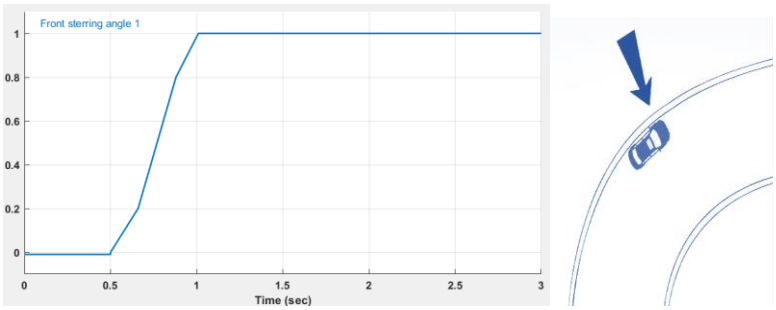

Fig.8 Front steering angle_1- Curve test.

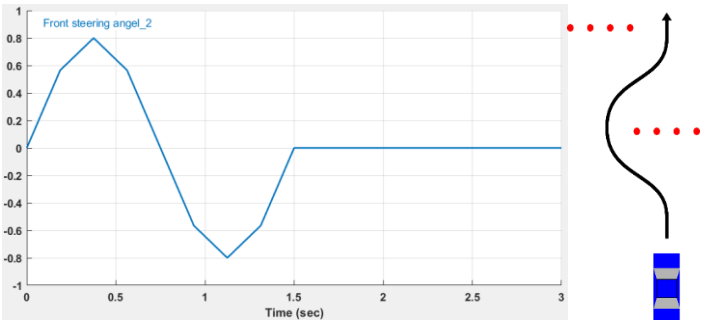

Fig.9 Front steering angle_2- Moose test.

These signals also represent inputs to the reference frame, which in turn generates the desired yaw rate and lateral slip angle signals as in Fig. 5. Model Matching Controller Block Diagram.

3. System analysis

Once the model and the parameters, it is possible to move on to the analysis phase. This phase includes the analysis of the system modes, structural properties, and the analysis of free and forced evolution. Analysis consists of studying the relationship between the inputs, state, and outputs of the system to understand and predict its behaviors.

3.1. Modal analysis

In this part, we analyze the eigenvalues of dynamic matrix A corresponding to Eq. 24 of the system. To calculate the eigenvalues, the roots of the characteristic polynomial are computed.

$$\det(\lambda I - A) = 0 \tag{38}$$

The parameters of the desired model A are determined from the original vehicle parameters and are shown in table 1.

Table.1. Vehicle and desired model parameters

Original vehicle	Desired model
$\boldsymbol{m}$ = 1562 kg	$\tau_\beta = 0.05\ sec$
$\boldsymbol{I_z}$ = 2630 kg m^2	$k_\beta = 0$
$\boldsymbol{a_f}$ = 1.104 m	$\tau_\gamma = 0.0375\ sec$
$\boldsymbol{a_r}$ = 1.421 m	$k_\gamma = 3.03\ sec^{-1}$
$\boldsymbol{c_f}$ = 42,000 N/rad	
$\boldsymbol{c_r}$ = 64,000 N/rad	
V = 80 k/h	

The eigenvalues are:

$$\lambda_1 = -3.0704 + 3.9962i$$

$$\lambda_2 = -3.0704 - 3.9962i$$

The eigenvalues are complex conjugates. The real part $\mathbb{R}e(\lambda i)$<0, i=1,2. Therefore the system is stable

3.2. Free evolution

This evolution corresponds to the behaviour of the states and outputs when the input is null, and the system only depends on the initial conditions.

Fig.10 shows the dynamic behavior of the system starting from different initial conditions for the slip angle and yaw rate:

$$x_0 = [0.65\ \ 0.12]$$

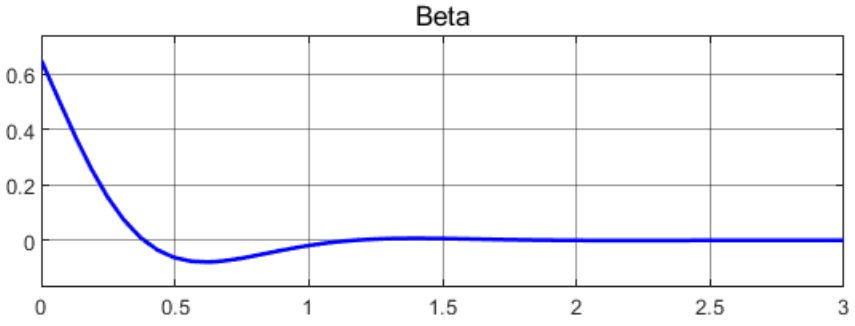

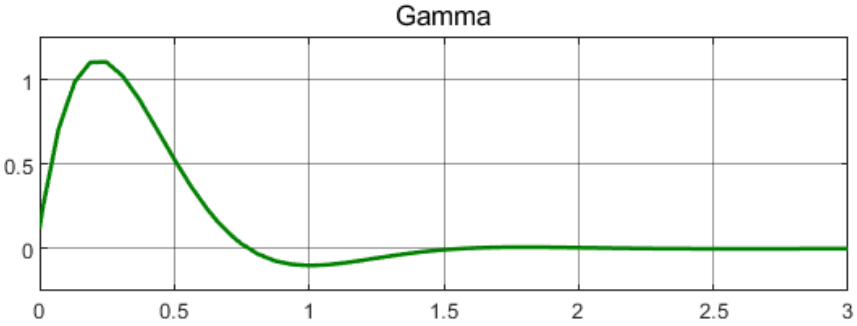

Fig.10. Free response for initial condition [0.065, 0.12]

As we can see in the picture below the state tends to zero “Equilibrium point” after a few seconds, this is because the system is asymptotically stable.

3.3. Force response

This corresponds to the response of the system because of inputs and when the initial conditions are 0. It is analyzed the case in which a step of amplitude equal to 0.0436 is applied to the input of the rear slip angle, and 1000Nm in direct yaw moment input for zero initial condition.

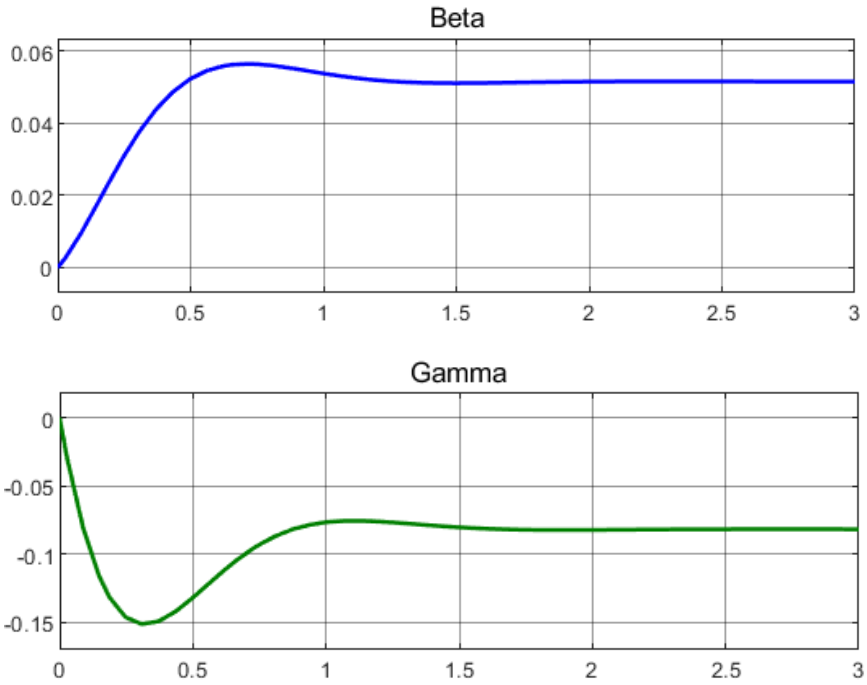

Fig.11. Force response for a step input of [0.04, 1000] corresponding to δr and *N* respectively.

It can be seen that both states react to inputs distinct from zero but tend toward a constant value in steady-state conditions.

3.4. Structural properties

The structural properties of LTI systems are necessary and sufficient conditions for the synthesis of control laws and observers.

Reachability and controllability are conditions for Input/State. Under these conditions is possible to design control laws of the state. these analyse if the actuators are well located and if these are sufficient. While Observability and constructability are conditions for State/Output. these concern the localization and number of sensors, under these conditions, it is possible to design observers.

Reachability

The reachability concept refers to the real possibility of being able to modifier the estate of the system acting on its inputs so that it assumes arbitrary conditions. To know if the system is reachable it is necessary to compute the reachability matrix which is related to matrices A and B in the following way.

$$R = [B\ AB\ A^2B\ \dots A^{n-1}B] \in R^{n\ x\ n.m} \quad (39)$$

Using *ctrb* command in MATLAB is possible to get the matrix R which is:

$$R = \begin{bmatrix} 1.8438 & 0 & 26.9506 & -0.0004 \\ -34.5795 & 0.0004 & 137.9995 & -0.0012 \end{bmatrix}$$

The system is completely reachable if and only if the rank of the reachable matrix is full rank, to certificate this, the rank command was used resulting in $rank(R) = 2$. It means that the system is completely reachable.

Reachability and Controllability in CT-case are the same, complete Reachability implies complete controllability and vice versa.

Observability

Observability is the property under which given a sequence of inputs $u(\mathrm{t})$ and sequence de outputs $y(\mathrm{t})$ it is possible estimate the initial condition $x(t_0)$ of the system.

It is said that a system is complete observable if the knowledge of inputs and outputs sequence allow to compute the initial state without errors. Besides, there are not indistinguishable states in the future.

the observability matrix is linked to A and B matrix in the following way:

$$O = \begin{bmatrix} C \\ CA \\ CA^2 \\ \vdots \\ CA^{n-1} \end{bmatrix} \in R^{p.n\ x\ n} \quad (40)$$

In the case of study, the observability matrix is:

$$O = \begin{bmatrix} 1 & 0 \\ 0 & 1 \\ -3.0538 & -0.9422 \\ 16.9490 & -3.0871 \end{bmatrix}$$

A linear system is complete reachable if and only if the observability matrix is full rank. Using MATLAB is verified that the $rank(O) = 2$, It means that the system is complete observable.

Constructability is a weaker condition than observability and consist in given a sequence of inputs $u(\mathrm{t})$ and $y(\mathrm{t})$ it is possible estimate $x(t)$ of the system. However, complete observability implies complete constructability. It can be said that in CT-case the constructability and observability are the same concept.

4. Linear Matrix Inequalities theory

The LMI (Linear Matrix Inequalities) is a very powerful tool in the field of control system theory. Because many problems in control theory, identification, signal processing, stability … etc can be recast or formulated as optimization problems with LMI constrains. These formulations are widely used for the efficiency on the numeric algorithms in terms of computational time. Often LMI are encounter in problems where the decision variables are matrices like Lyapunov stability method for linear systems.

Linear Matrix Inequality is defined as an affine combination of matrices constrained to be positive or negative definite, formally.

Given a set of square and symmetric matrices $F_i = F_i^T \in \mathbb{R}^{nxn}, i = 0,1 \dots m$ and a vector $x \in \mathbb{R}^m$, a LMI is defined as:

$$F(x) = F_0 + \sum_{i=1}^{m} (x_i F_i) < 0 \; or > 0 \qquad (41)$$

LMS are very important as they allow defining convex constrains. Therefore, each time that a control problem is defined into a set of LMI constrains, our problem has been reduced to one of convex optimization.

Often when working with LMI, individual variables are not explicitly stated, but matrix of variables are used. Similar, when there is a set of LMIs it is possible to reduce this to a single LMI using matrix notation, that is, a set of satisfiable LMIs with the same properties as a single LMI.

$$\begin{cases} F^{(1)}(x) < 0 \\ F^{(2)}(x) < 0 \\ \dots \\ F^{(k)}(x) < 0 \end{cases} \leftrightarrow \begin{bmatrix} F^{(1)}(x) & \dots & 0 \\ \dots & \dots & \dots \\ 0 & \dots & F^{(k)}(x) \end{bmatrix} \qquad (42)$$

4.1. LMI Stability

A way to prove stability is using *Lyapunov Algebraic equation*. This theorem state that the system $\dot{x} = Ax$ is asymptotical stable if and only if, for some symmetrical matrix $Q = Q^T > 0$, the ALE admits a unique solution $P = P^T > 0$ such that:

$$A^T P + PA = -Q \qquad (43)$$

Using LMI and Lyapunov stability criterion the problem can be stated as following:

Let $V(x) = x^T P x \, , P \in \mathbb{R}^{nxn}, P = P^T > 0$ be a positive define quadratic Lyapunov function. The sufficient condition for asymptotical stability is $\dot{V}(x) < 0 \quad \forall x \in \mathbb{R}^n / 0_x$

In LIM term must be verified the conditions:

$$\exists P = P^T > 0 \qquad st \qquad A^T P + PA < 0 \qquad (44)$$

Using Schur Complement it is translated in the following LMI:

$$\begin{bmatrix} -P & 0 \\ 0 & A^T P + PA \end{bmatrix} < 0 \qquad (45)$$

Which is a feasibility problem of LMI with P unknown. Taking advantage of MATLAB, it is possible to determine a matrix P that satisfies the Lyapunov condition. The result obtained is:

$$P = 1.0e-11 \begin{bmatrix} 0.1460 & -0.0174 \\ -0.0174 & 0.0114 \end{bmatrix}$$

The result of the Eq.45 is:

$$1.0\text{e}-10 \begin{bmatrix} -0.1483 & 0.0163 \\ 0.0163 & -0.0038 \end{bmatrix}$$

The eigenvalues resulting of this matrix are:

$$1.0\text{e}-10 \begin{bmatrix} -0.1501 \\ -0.0020 \end{bmatrix}$$

As shown, the eigenvalues of the matrix are negative, therefore the matrix is negatively defined. Hence, the system is asymptotically stable as we discovered in the previous analysis with the classical technique.

4.2. LMI region

It is well known that the dynamic properties of a linear, time-invariant system are determined by the location of the poles of its transfer function in the complex plane. For second order systems, there is a particularly simple relationship between the pole location and damping ratio, rise time and settling time. Standard methods are available to find a controller that places the poles in specified locations in the complex plane. However, it is not obvious where exactly the poles of the closed-loop system should be located to achieve good performance: the required control effort is larger when the poles

are moved far away from their original locations, and in the presence of transfer function, zeros also have an effect on the response. In practice the designer often works on specifications that include a minimum damping ratio and a minimum speed of response, and it is desired to find the best controller (in terms of a suitable performance index) that satisfies these constraints. The constraints can be expressed as a region in the complex plane where the closed-loop poles should be located. A typical pole conical region $\boldsymbol{S(\alpha,r,\theta)}$ in the complex plane is shown in Fig. 12. The condition that the poles of a system are located within a given region in the complex plane can be formulated as an LMI constrains.

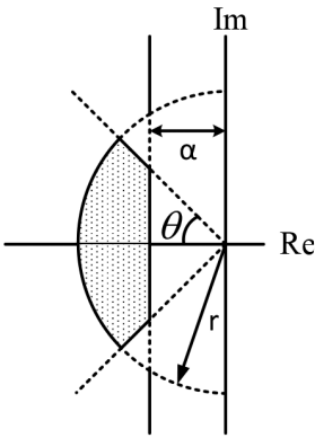

Fig.12 Region S(α, r, θ), composed by the intersection of three convex LMI regions.

Where:

α: Real part of cone tip. It is related with the setting time.

θ: Angle of the cone. It is related to the overshoot.

r: Cone radius. It is related to the natural pulsation.

In particular, $\boldsymbol{\alpha}$ is the largest of the real parts of the numbers belonging to the cone, $\boldsymbol{\theta}$ is the largest of the phases of these numbers, and $\boldsymbol{r}$ is the largest of their modules. Based on these considerations, the eigenvalues of A are contained in the conic region characterized by:

$$\begin{aligned} \alpha &= -max\big(Re(\lambda)\big);\ \lambda \in sp(A) \\ \theta &= max\big(\angle(\lambda)\big);\ \lambda \in sp(A) \\ r &= max(||\lambda||);\ \lambda \in sp(A) \end{aligned} \tag{46}$$

The results given by MATLAB are:

$$\alpha = 3.0704$$
$$\theta = 2.2259$$
$$r = 5.0395$$

Using LMI, it is possible verify the correctness of the result already found.

In fact, let $\boldsymbol{S(\alpha,r,\theta)}$ be a conic sector, the matrix A has the eigenvalues all internal of $\boldsymbol{S(\alpha,r,\theta)}$ if and only if $\exists\ P$ such that Eq 47 is satisfied.

$$\begin{cases} [PA + A^{\mathbf{T}}P + \mathbf{2}\alpha P] < 0 \\ \begin{bmatrix} -rP & PA \\ A^TP & -rP \end{bmatrix} < 0 \\ \begin{bmatrix} \sin(\theta)(PA + A^{\mathbf{T}}P) & \cos(\theta)(PA - A^{\mathbf{T}}P) \\ \cos(\theta)(-PA + A^{\mathbf{T}}P) & \sin(\theta)(PA + A^{\mathbf{T}}P) \end{bmatrix} < 0 \end{cases} \tag{47}$$

Using MATLAB, it is identified the matrix $P = P^T > 0$ such that the above condition is satisfied, then it confirms that the values of $(\boldsymbol{\alpha,r,\theta})$ are correct

$$P = 1.0\text{e} - 14 \begin{bmatrix} 0.1604 & -0.0180 \\ -0.0180 & 0.0067 \end{bmatrix}$$

4.3. Norms.

One way to measure the performance of a control system is in terms of the size of certain signals of interest. For example, the performance of the tracking system could be measured by the size of the error signals.

An important concept for the development of this project is to introduce the notion of norms for systems transfer function. Also, it is important understand which norm is appropriate depending on the situation, for which refer to Table.2 and Table.3.

Norms of LTI systems.

Consider the simple case:

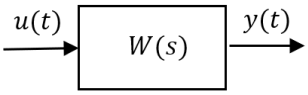

Let $y(t)\epsilon\mathbb{R}^p$ be the system response to a causal input $u(t)\epsilon\mathbb{R}^m$. with the following representation

$$Time - domain:\ y(t) = \int_{-\infty}^{t} W(t-\tau)u(\tau)d\tau\,, \qquad W(t) \in \mathbb{R}^{pxm} \tag{48}$$

$$Frecuency - domain: \qquad \hat{y}(s) = W(s)\,\hat{u}(s), \qquad W(s) \in \mathbb{R}(s)^{pxm} \tag{49}$$

When dealing with LIT systems, the transfer functions matrices are Real rational and under certain conditions can be seen as elements of RH_2 or RH_∞. Then, the space and their norms are the natural candidates to measure the size of the system. And we would like to find an expression for the induces norm W such that:

$$\|y\|_p \leq \|W\|_q \|u\|_p, \ \ \forall u \in \mathcal{L}_p \tag{50}$$

In the case of the scalar systems the norms of interest are:

$$\mathcal{L}_1 - norm \qquad \|w\|_{\mathcal{L}_1} = \int_0^\infty |W(t)|dt \tag{51}$$

$$H_2 - norm \qquad \|w\|_{H_2} = \left[\frac{1}{2\pi}\int_{-\infty}^{\infty} |W(jw)|^2 dw\right]^{1/2} \tag{52}$$

$$H_\infty - norm \qquad \|w\|_{H_\infty} = sup_w |W(jw)| \tag{53}$$

Based on the above norms, the spaces where these transfer functions are bounded are the following:

$$R\mathcal{L}_1 = \{W(S)\ s.t\ W(t) \in \mathcal{L}_p\ (BIBO\ stability)\} \tag{54}$$

$$RH_2 = \{W(S)\ s.t\ W(S)\ stric\ poper, without\ poles\ on\ Re(s) \geq 0\} \tag{55}$$

$$RH_\infty = \{W(S)\ s.t\ W(S)\ \ poper, without\ poles\ on\ Re(s) \geq 0\} \tag{56}$$

In the multiple variable case $W(s) \in \mathbb{R}(s)^{pxm}$, $W(t) \in \mathbb{R}^{pxm}$ the above norms become:

$\mathcal{L}_1 - norm$, It is called the *peak-to-peak gain* and relates the max amplitude of the output with the max amplitude of the input.

$$\|w\|_{\mathcal{L}_1} = \max_{1\leq i\leq p} \int_0^\infty \sum_{j=1}^{m} \left|W_{ij}(t)\right| dt \tag{57}$$

$$where\ w(t) = \left[W_{ij}(t)\right]$$

$H_2 - norm$, role of $L_2 - L_\infty$ induced gains. Relate max amplitude of output with energy of input.

$$\|w\|_{H_2} = \left[\frac{1}{2\pi}\int_{-\infty}^{\infty} tr\{W^T(-jw)W(jw)\}dw\right]^{1/2} \tag{58}$$

$$where\ w^*(jw) = w^T(-jw)$$

$H_\infty - norm$, It is called *RMS gain* and relates the energy/power of the output with the energy/output of the input.

$$\|w\|_{H_\infty} = sup_w \bar{\sigma}(W(jw)) \quad (59)$$

$$where\ \bar{\sigma}(W(jw) = \sqrt{\bar{\lambda}(w^T(-jw)\big(W(jw)\big)}\ , \bar{\lambda} = \max eigenvalue$$

Use the systems norms as induced norms.

The question of interest in this section is: if we know how big the input is, how big is the output going to be? Consider a linear system with input u, output y, and transfer function $\widehat{W}$, assumed stable and strictly proper. The results are summarized in two tables below.

In the case of known inputs

Table.2. induced norms with known inputs.

$y(t)$ \ $u(t)$	*Dirac impulse* $u(t) = \delta(t)$	*sinusoidal* $u = \sin(wt)$	*White noise* $u(t) = w{\sim}(0, {\sigma_u}^2)$
$\|y\|_2$	$\|w\|_{H_2}$	∞	∞
$\|y\|_\infty$	$\|w\|_{H_\infty}$	$\|W(jw)\|$	$\leq \infty$
$\|y\|_{RMS}$	0	$\frac{1}{\sqrt{2}}\|W(jw)\|$	${\sigma_y}^2 = \|w\|_{H_2}^2 {\sigma_u}^2$

In the case when $u(t)$ is unknown, but it belongs to a specific signal space.

$$\mathcal{L}_p = \{u(t) \in \mathcal{L}_p\ iff\ \|u\|_p < \infty\}$$

The following induced norms holds.

Table.3. induced norms with unknow inputs.

$y(t)$ \ $u(t)$	$\mathcal{L}_2$ $\|u\|_2$	$\mathcal{L}_\infty$ $\|u\|_\infty$	$\mathcal{L}_{RMS}$ $\|u\|_{RMS}$
$\|y\|_2$	$\|w\|_{H_\infty}$	∞	∞
$\|y\|_\infty$	$\|w\|_{H_2}$	$\|w\|_{\mathcal{L}_1}$	$\leq \infty$
$\|y\|_{RMS}$	0	$\leq \|w\|_{H_\infty}$	$\|w\|_{H_\infty}$

A typical application of these tables is as follows. Suppose that our control analysis or design problem involves, among other things, a requirement of disturbance attenuation: The controller system has a disturbance input, say u, whose effect on the plant output, say y, should be small. Let W denote the impulsive response from u to y. The controller system will be required to be stable, so the transfer function $\widehat{W}$ will be stable. Typically, it will be strictly proper, too (or at least proper).

The tables 2 and 3 tables tell us how much u affects y according to various measures. For example, if u is known to be a sinusoidal with fixed frequency, then the second column of the table 2 gives the relative size of $according$ to three measurements.

5. Control design

The state static feedback law is of the type:

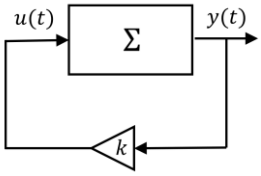

Basic regulation problem, the given plant $\dot{x}(t) = Ax(t) + Bu(t)$, consist in determining a matrix $k \in \mathbb{R}^{mxn}$ such that, the control law $u(t) = kx(t)$ makes the close loop system $\dot{x}(t) = (A + Bk)x(t)$ asymptotically stable

We want to create a static controller which, in addition to guaranteeing the asymptotic stability of the system, assure the specifications on the induced norms of the system. Therefore, starting from the open loop system described by the following equations:

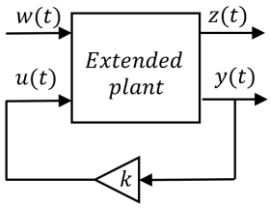

$$\sum ol : \begin{cases} \dot{x}(t) = Ax(t) + B_1u(t) + B_2w(t) \\ z_\infty(t) = C_1x(t) + D_{11}w(t) + D_{12}u(t) \\ z_2(t) = C_2x(t) + D_{22}u(t) \\ z_1(t) = C_3x(t) + D_{31}w(t) + D_{32}u(t) \end{cases} \quad (60)$$

Where z_∞, z_2, z_1 are the control objectives or the performance outputs on which is necessary to find an optimal k so that the feedback system Eq.61 results in the best possible performance.

$$\Sigma cl: \begin{cases} \dot{x}(t) = (A + B_1k)x(t) + B_2w(t) \\ Z_\infty = (C_1 + D_{12}k)x(t) + D_{11}w(t) \\ Z_2 = (C_2 + D_{22}k)x(t) \\ Z_\infty = (C_3 + D_{32}k)x(t) + D_{31}w(t) \end{cases} \quad (61)$$

The control actions have been projected to make a zero regulation of the error, the states considered to regulate are the errors between the reference signals (lateral slip angle and yaw rate produced by the model generator) and the output of the system. As previously specified in the Model Matching Controller, feedback gain is implemented first and successively implemented the feedforward gain.

For feedback gain, the control action will be aimed at minimizing the effects of the disturbance and will lead to setting the tracking error to zero. For the objective are proposed different types of controls which are described in the following section.

5.1. H_2 - Optimal Control

The objective of this control is to minimize the norm H_2, i.e., the amplitude of the output of interest, considering the input signals as limited in energy, through the following relationship:

$$\|y\|_\infty \leq \|W\|_{H_2}\|u\|_2 \quad (62)$$

The zero regulation of the states (errors signals) is the main objective of the control design, following this idea the controller H_2 allows to have outputs with limited amplitudes. Therefore, the controller that make the closed loop $(A + Bk)$ asymptotically stable and minimizes the $H_2 - norm$ is obtained by stablishing the following LMI condition:

$$\begin{cases} [x^*, y^*] = \min_{X,Q,Y,\gamma} \gamma \\ s.t \\ \begin{bmatrix} AX + B_1Y + (AX + B_1Y)^T & B_2 \\ B_2^T & -I \end{bmatrix} < 0 \\ \begin{bmatrix} Q & (C_2X + D_{22}Y) \\ (C_2X + D_{22}Y)^T & X \end{bmatrix} > 0 \\ tr\{Q\} < \gamma \\ X > 0 \\ Q > 0 \end{cases} \quad (63)$$

If a solution exists, it is unique and the optimal control H_2 is given by.

$$k_2^* = y^* x^{*-1} \quad (64)$$

The results using MATLAB are:

$$k_2^* = 1.0\text{e}+5 \begin{bmatrix} -1.188317147747838 & 4.390297532271924 \\ 0.126468185257715 & -0.467196421380189 \end{bmatrix}$$

The related eigenvalues of the close loop plant are:

$$eig\ H_2 = 1.0\text{e}+7 \begin{bmatrix} -0.00000024147542 \\ -1.540053738165996 \end{bmatrix}$$

And the stability of the controller is verified.

Simulations

In the H_2 control it is not possible to follow an input reference, but as the controller has been designed so that the main objective is to make a zero regulation of the error, therefore, the simulation is performed according the two disturbance input signals: curve and moose test.

Moose test

The Fig.12 shown the response of the system due to the H_2-controller and without controller for a disturbance related to moose test in the front steer angle.

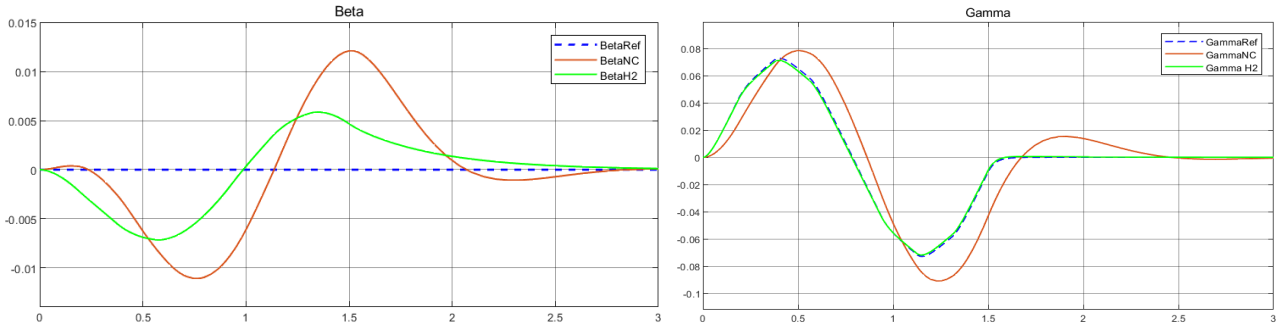

Fig.13 $\boldsymbol{\beta}$ Side slip angle of the vehicle body [rad] and $\boldsymbol{\gamma}$ Yaw rate of the vehicle body [rad/s]

From Fig.13 it is possible to notice that the side slip angle of the control system “BetaH2” is more contained with respect to the non-controller one “BetaNC”. Additionally, the controlled yaw rate “GammaH2” tend to follow the desired reference signal.

The Fig.14 shown the corresponding errors regulated by the H_2-controller.

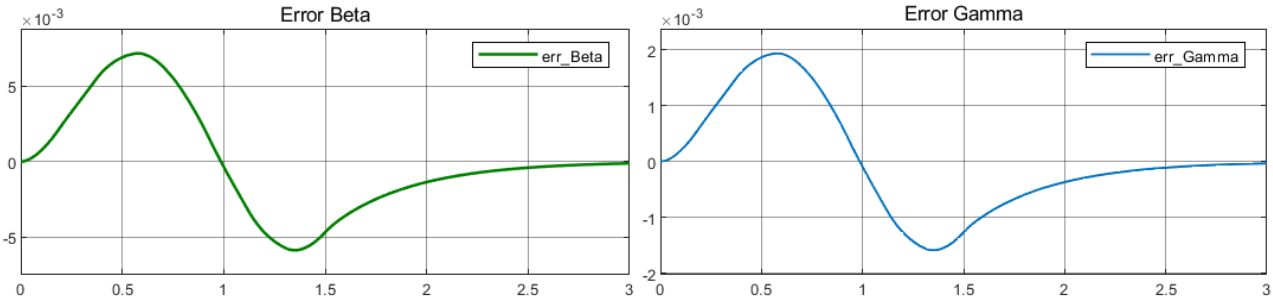

Fig.14 tracking errors of the states

The Fig.15 shown the input signals corresponding to Direct yaw moment and rear wheel steering angle generated by the H_2-controller.

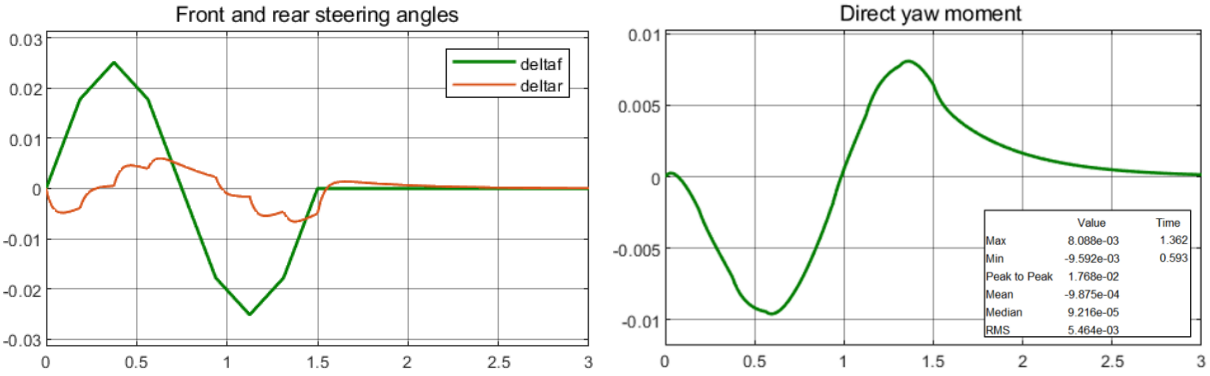

Fig.15 Rear wheel steering angle Direct yaw moment inputs

The first part shown the front and rear steering angle when the vehicle is moving at 80 km/h, the second part shown the Direct yaw moment due to the H_2-controller and it reaches a maximum value of 8.088e-3 and a minimum value of -9.592e-3 [Nm].

Looking at the results of the yaw rate versus the front steering wheel angle shown in Fig. 15, it can be seen that the response becomes very close to the desired response when using the model matching controller with H_2-controller. Moreover, the phase delay between the yaw rate and steering wheel input greatly decreases so that the handling performance can be much improved for the driver.

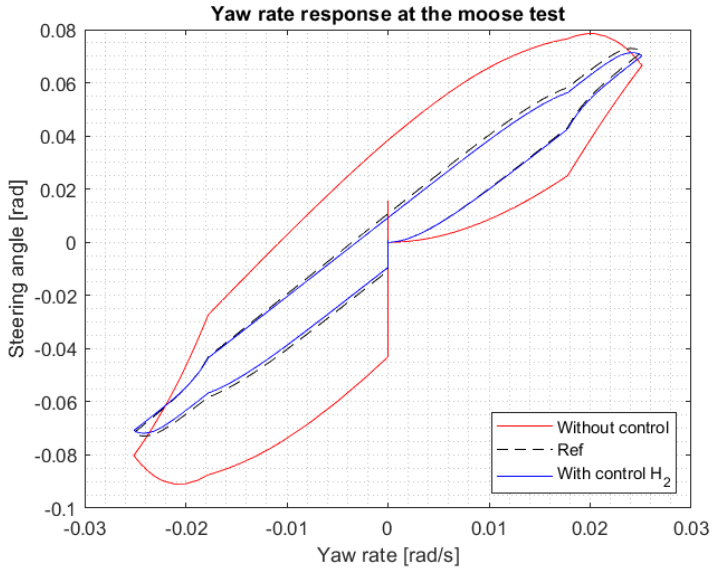

Fig.16 Yaw rate versus steering wheel angle

Curve test

Now, the result of the controlled system when the disturbance is related to curve test in the front steer angle are presented.

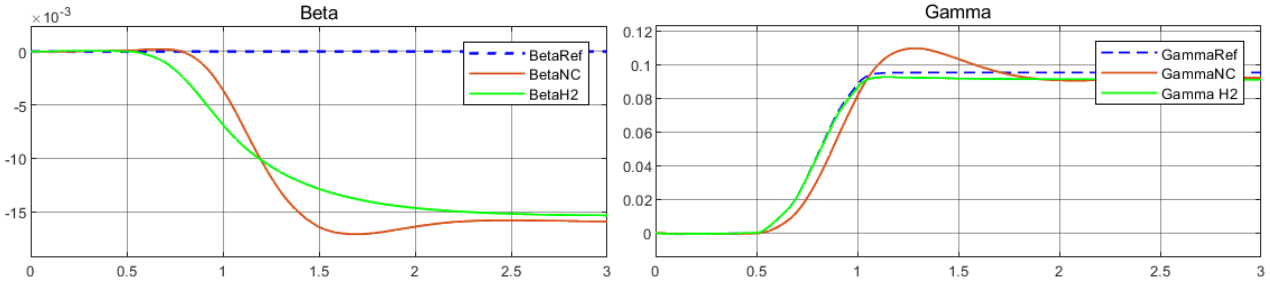

Fig.17 $\boldsymbol{\beta}$ Side slip angle of the vehicle body [rad] and $\boldsymbol{\gamma}$ Yaw rate of the vehicle body [rad/s] for curve test

In this case Beta does not return to zero because it is sumulated a continous steering angle along the time.

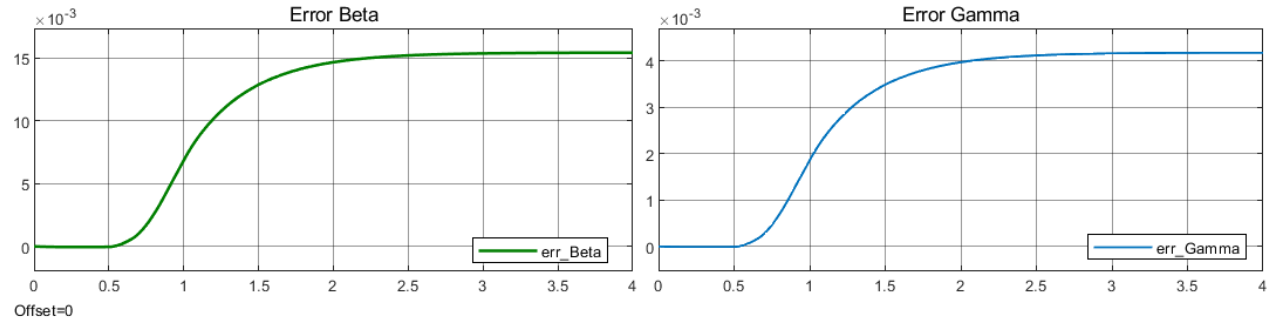

Fig.18 tracking errors of the states

In this prove the errors are greater with respect to those obtained in the moose test but it is observed that the erros converge to stable conditions.

The Fig.19 shown the input signals corresponding to Direct yaw moment and rear wheel steering angle generated by the H_2-controller. The direct yaw moment reaches a maximum value of 1.540e-4 and a minimum value of -1.950e-2 [Nm]

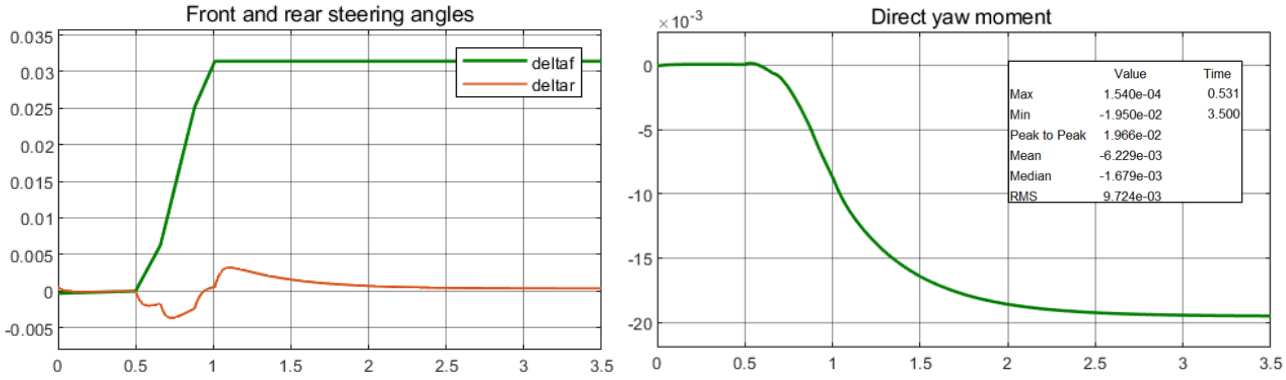

Fig.19 Rear wheel steering angle Direct yaw moment inputs curve test

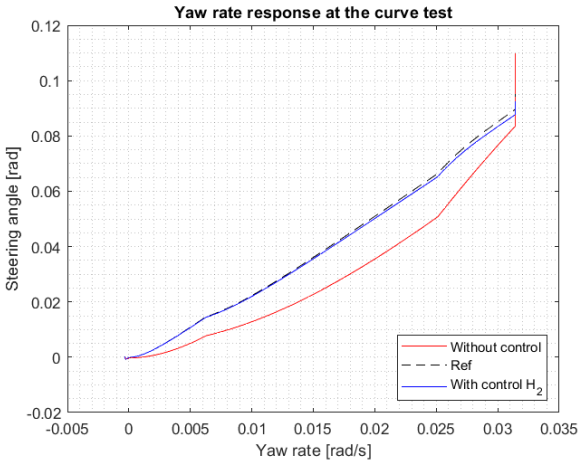

Fig.20 Yaw rate versus steering wheel angle

5.2. $\boldsymbol{H}_\infty$ - Optimal Control

The objective of this control is to minimize the norm H_∞ of the transfer function $W(s)$. From the induced norms in the table 3 is possible found the relationship that link the input and output with H_∞ norm

$$\|y\|_2 \leq \|W\|_{H_\infty}\|u\|_2 \tag{65}$$

Minimizing the H_∞ norm result in minimize the energy of the output. In fact, H_∞ control, is a wide used technique in control system theory to design robust and optimal controllers. Due to, Its main objective is to ensure satisfactory performance of the control system even in the presence of disturbances, uncertainties in system parameters, and noise. In other words, the goal is to minimize the influence of the most unfavorable disturbances while ensuring a desired response for the signals of interest.

Given a finite dimensional LTI system, it is necessary to find static feedback of the state such that in closed loop the transfer function *W* has the norm H_∞ smaller than an upper limit fixed a priori.

$$\|W\|_{H_\infty} < \gamma \tag{66}$$

It is wanted to minimize the output of the error with respect to the disturbance according to the Eq.31. Then, it is possible set the following LMI problem:

$$\begin{cases} [x^*, y^*] = \min_{X,Y,\gamma} \gamma \\ s.t \\ \begin{bmatrix} AX + B_1Y + (AX + B_1Y)^T & B_2 & (C_1X + D_{12}Y)^T \\ B_2^T & -\gamma I & D_{11}^T \\ (C_1X + D_{12}Y) & D_{11} & -\gamma I \end{bmatrix} < 0 \\ \gamma > 0 \\ X = X^T > 0 \end{cases} \tag{67}$$

If a solution exists, it is unique and the optimal control H_∞ is given by.

$$k_\infty^* = y^* x^{*-1} \tag{68}$$

The results using MATLAB are:

$$k_\infty^* = 1.0\text{e}+6 \begin{bmatrix} -0.000374079707664 & 0.000694466838637 \\ -1.815197802548653 & -0.114692304741959 \end{bmatrix}$$

The related eigenvalues of the close loop plant are:

$$eig\ H_\infty = 1.0\text{e}+4 \begin{bmatrix} -0.003962464811373 \\ -2.471414346455699 \end{bmatrix}$$

And the stability of the controller is verified.

Simulations

Moose test

The Fig.21 shown the response of the system due to the H_∞-controller and without controller for a disturbance related to moose test in the front steer angle.

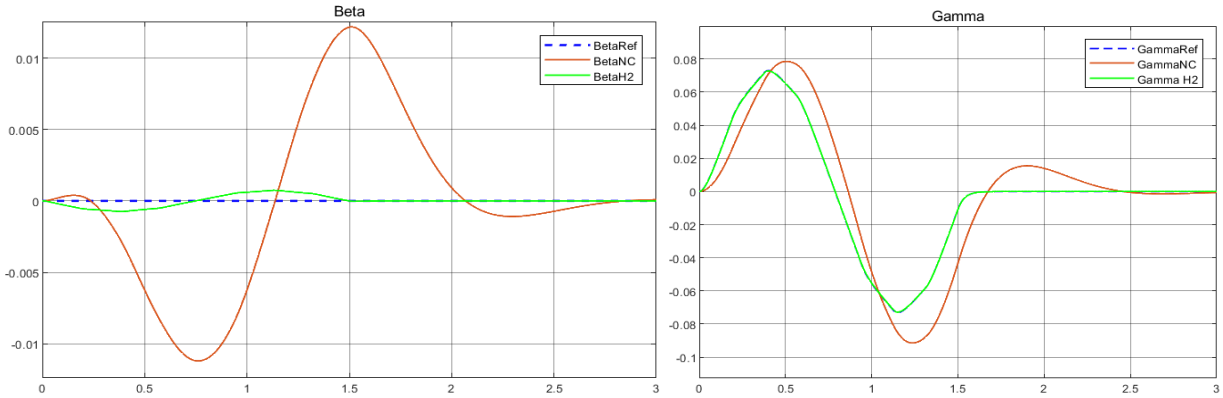

Fig.21 $\boldsymbol{\beta}$ Side slip angle of the vehicle body [rad] and $\boldsymbol{\gamma}$ Yaw rate of the vehicle body [rad/s]

it can be highlighted that the lateral slip angle $\boldsymbol{\beta}$ is much more contained with respect to the uncontrolled one (BetaNC), while the yaw rate tends to follow the reference signal almost perfectly.

The Fig.22 shown the corresponding errors regulated by the H_∞-controller.

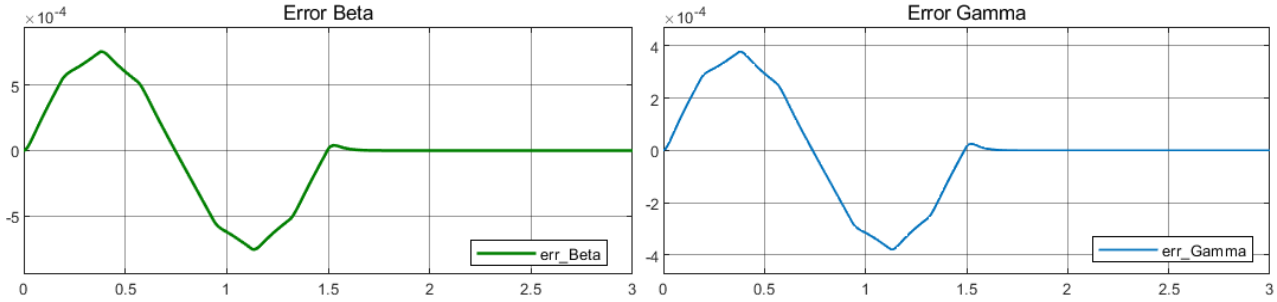

Fig.22 tracking errors of the states

The Fig.23 shown the input signals corresponding to Direct yaw moment and rear wheel steering angle generated by the H_∞-controller.

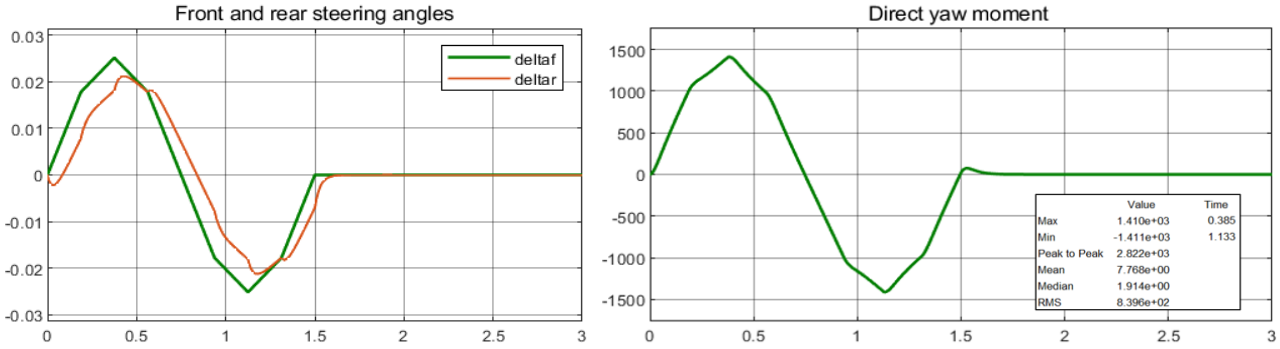

Fig.23 Rear wheel steering angle Direct yaw moment inputs

The first part shown the front and rear steering angle when the vehicle is moving at 80 km/h, the second part shown the Direct yaw moment due to the H_∞-controller and it reaches a maximum value of 1410 and a minimum value of -1411e $[Nm]$. From the simulations we can observe that the control input signal corresponding to the direct yaw moment is very high with respect to the control signal in H_2This is because the H_2 control allows to have outputs with limited outputs.

Fig.24 refers to the system response taking into account the yaw rate as a function of the front wheel steering angle.

Fig.24 Yaw rate versus steering wheel angle

Looking at the results of the yaw rate versus the front steering wheel angle shown, it can be seen that the response becomes almost perfectly to the desired response when using the model matching controller with H_∞--controller.

Curve test

Now, the result of the controlled system when the disturbance is related to curve test.

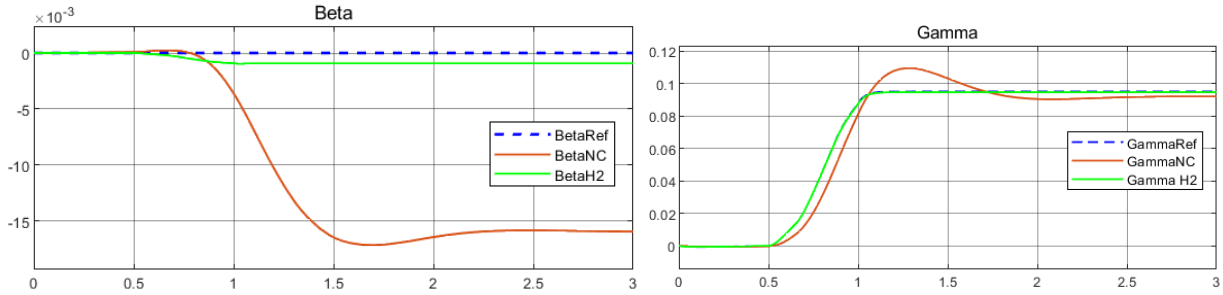

Fig.25 $\boldsymbol{\beta}$ Side slip angle of the vehicle body [rad] and $\boldsymbol{\gamma}$ Yaw rate of the vehicle body [rad/s] for curve test

In this case Beta is near to zero by the good performance on the H_∞-controller.

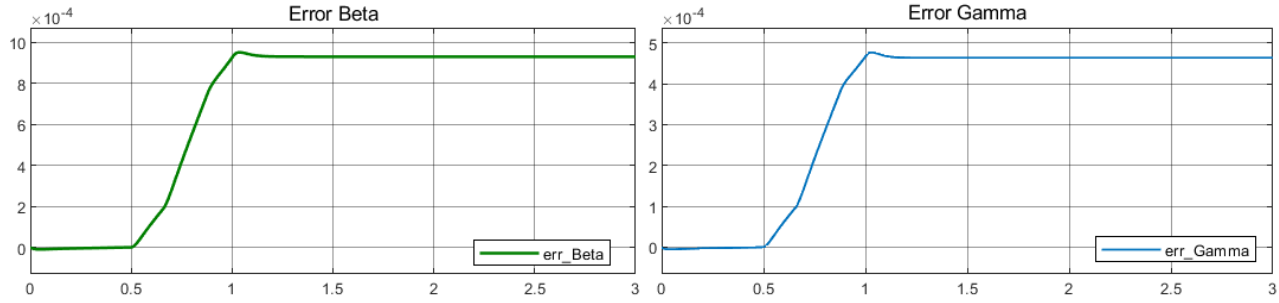

Fig.26 tracking errors of the states, curve test

In this prove the errors shown in the Fig.26 are greater with respect to those obtained in the moose test but it is observed that the erros converge to stable conditions with a little diference from zero.

The Fig.27 shown the input signals corresponding to Direct yaw moment and rear wheel steering angle generated by the H_∞-controller. The direct yaw moment reaches a maximum value of 1781 and a minimum value of -1880 [Nm]

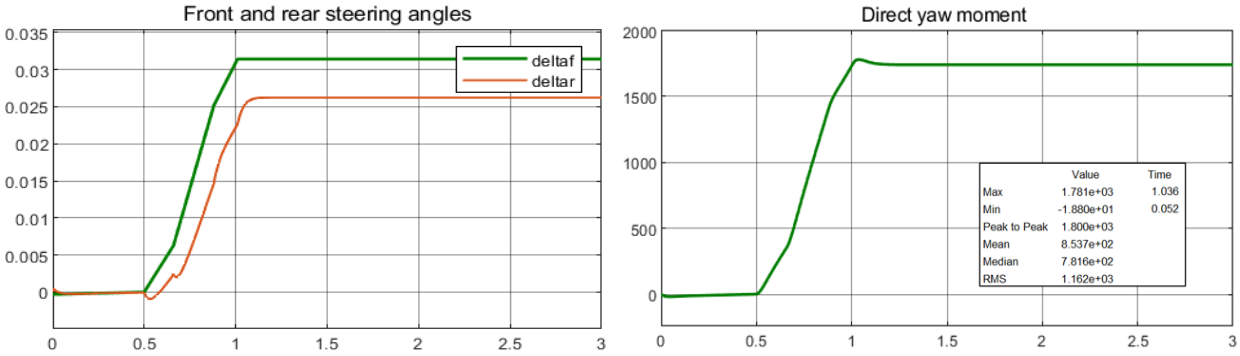

Fig.27 Rear wheel steering angle Direct yaw moment inputs curve test

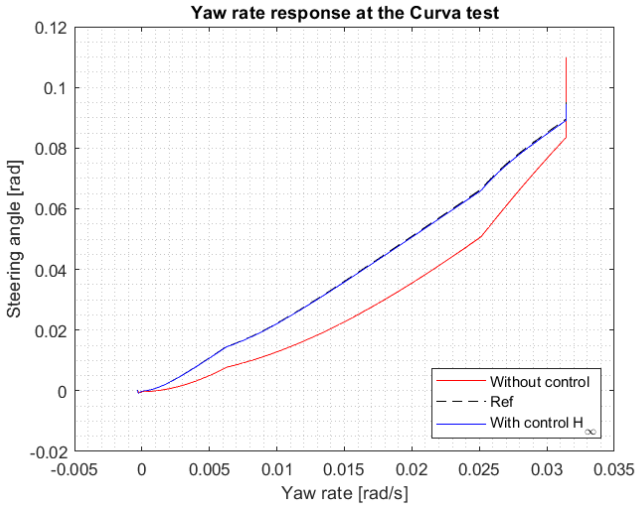

Fig.28 Yaw rate versus steering wheel angle curve test

5.3. L_1 - Optimal Control

The objective of this control is to minimize the norm L_1 of the transfer function $W(s)$. From the induced norms in the table 3 is possible found the relationship that link the input and output with L_1 norm

$$\|y\|_\infty \leq \|W\|_{L_1}\|u\|_\infty \tag{69}$$

This induced norm relates to the amplitude of the output of interest, also considering a small amplitude of the control signal. The zero regulation of the states (errors signals) is the main objective of the control design, following this idea the controller L_1 allows to have outputs with limited amplitudes. Therefore, the controller that make the closed loop $(A + Bk)$ asymptotically stable and minimizes the $L_1 - norm$ is obtained by stablishing the following LMI condition:

$$\begin{cases} [x^*, y^*] = \min\limits_{X,Y,\gamma,\mu} \gamma \\ s.t \\ \begin{bmatrix} \lambda X & 0 & (C_3X + D_{32}Y)^T \\ 0 & (\gamma-\mu)I & D_{31}^T \\ (C_3X + D_{32}Y) & D_{31} & -\gamma I \end{bmatrix} < 0 \\ \begin{bmatrix} AX + B_1Y + (AX + B_1Y)^T + \lambda X & B_2 \\ B_2^T & -\mu I \end{bmatrix} > 0 \\ \gamma > 0 \\ X = X^T > 0 \end{cases} \tag{70}$$

If a solution exists, it is unique and the optimal control H_∞ is given by.

$$k_1^* = y^* x^{*-1} \tag{71}$$

The results using MATLAB are:

$$k_1^* = 1.0\text{e}+05 \begin{bmatrix} -0.001118657057639 & 0.002294799468037 \\ 3.330564544292433 & -6.800341188804528 \end{bmatrix}$$

The related eigenvalues of the close loop plant are:

$$eig\ L_1 = 1.0\text{e}+06 \begin{bmatrix} -0.002621073106717 \\ -8.403639148287896 \end{bmatrix}$$

And the stability of the controller is verified.

Simulations

Moose test

The Fig.29 shown the response of the system due to the L_1-controller and without controller for a disturbance related to moose test in the front steer angle.

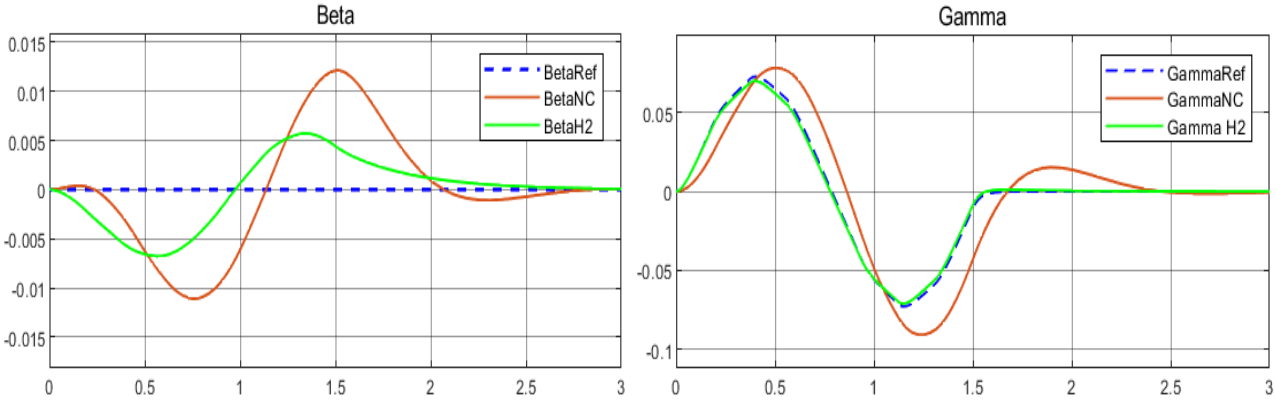

Fig.29 $\boldsymbol{\beta}$ Side slip angle of the vehicle body [rad] and $\boldsymbol{\gamma}$ Yaw rate of the vehicle body [rad/s]

it can be highlighted that the lateral slip angle $\boldsymbol{\beta}$ is more contained with respect to the uncontrolled one (BetaNC), while the yaw rate tends to follow the reference signal.

The Fig.30 shown the corresponding errors regulated by the L_1-controller.

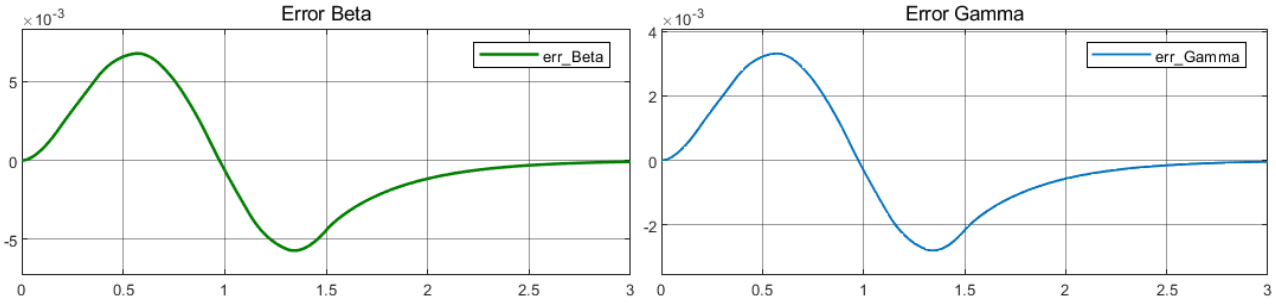

Fig.30 tracking errors of the states

The Fig.31 shown the input signals corresponding to Direct yaw moment and rear wheel steering angle generated by the L_1-controller.

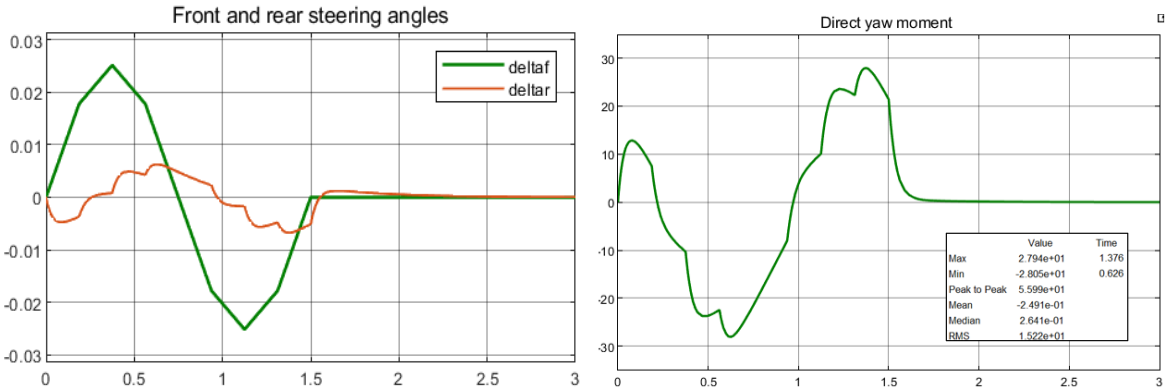

Fig.31 Rear wheel steering angle Direct yaw moment inputs

The first part shown the front and rear steering angle when the vehicle is moving at 80 km/h, the second part shown the Direct yaw moment due to the L_1-controller and it reaches a maximum value of 27.94 and a minimum value of -28.05 $[Nm]$.

Fig.32 refers to the system response taking into account the yaw rate as a function of the front wheel steering angle.

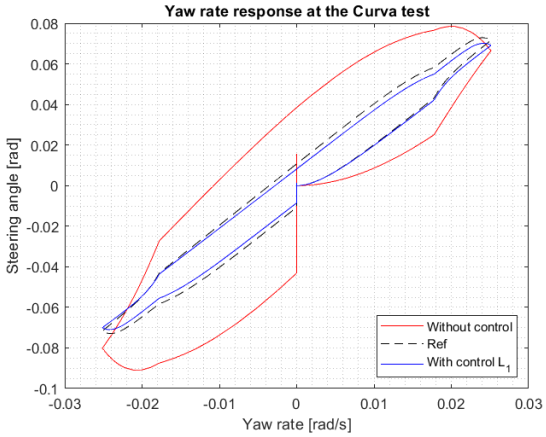

Fig.32 Yaw rate versus steering wheel angle

Looking at the results of the yaw rate versus the front steering wheel angle shown, it can be seen that the response becomes near to the desired response when using the model matching controller with L_1-controller.

Curve test

Now, the result of the controlled system when the disturbance is related to curve test.

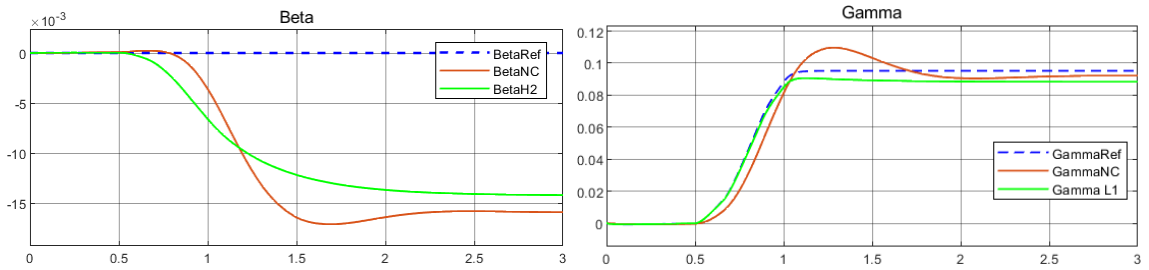

Fig.33 $\boldsymbol{\beta}$ Side slip angle of the vehicle body [rad] and $\boldsymbol{\gamma}$ Yaw rate of the vehicle body [rad/s] for curve test

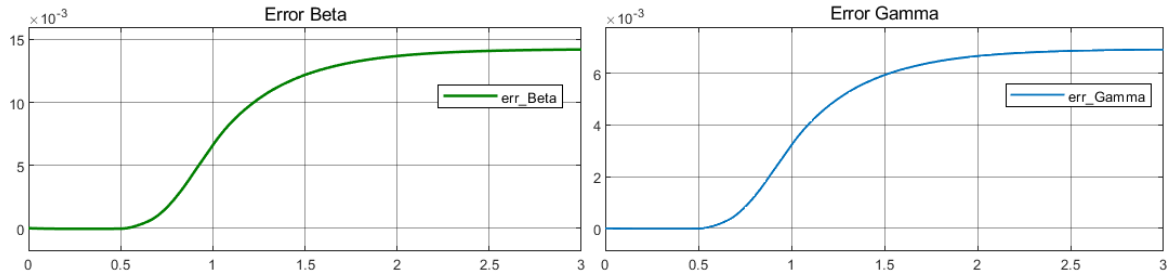

Fig.34 tracking errors of the states, curve test.

In this prove the errors shown in the Fig.23 are greater with respect to those obtained in the moose test but it is observed that the erros converge to stable conditions with a little diference from zero.

The Fig.35 shown the input signals corresponding to Direct yaw moment and rear wheel steering angle generated by the L_1-controller. The direct yaw moment reaches a maximum value of 8.280 and a minimum value of -24.79 $[Nm]$.

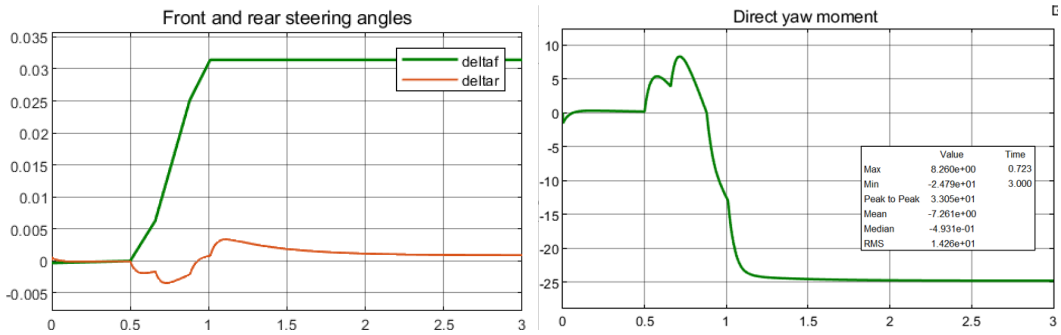

Fig.35 Rear wheel steering angle Direct yaw moment inputs, curve test.

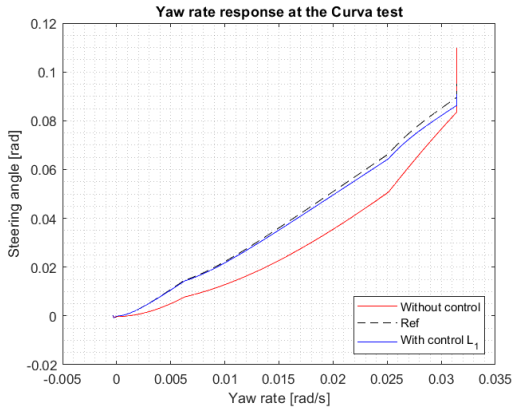

Fig.36 Yaw rate versus steering wheel angle curve test

5.4. *LQ*-Optimal control

This control unlike the previous ones does not minimize a induced norm instead it minimize a cost function.

Consider the system described in the Eq.22, the aim is to find a state feedback control $u(t) = kx(t), k \in \mathbb{R}^{mxn}$ that stabilize the system and minimize the following cost function.

$$J = \int_0^\infty x^T(t)Qx(t) + u^T(t)Ru(t)dt \tag{72}$$

With the following assumptions R and Q are symmetric and positive defined matrices the matrices A, B must be stabilizable. The first term of cost J measures the energy of the state (energy of the evolution), while the second term measure the energy of the input. The smaller the sum of these two contributions, the lower the value of the cost J: the objective of the LQ control is precisely minimize both terms. However, the terms imposer opposition to the other, in fact, minimize the energy of the input u leads to a deterioration of the system performance consequently produce an increase in the states energy.

Formulation of the LQ control in terms of LMI:

$$\begin{cases} [x^*, y^*] = \min_{X,Y} \gamma \\ s.t \\ \begin{bmatrix} AX + B_1Y + (AX + B_1Y)^T & X^T & Y^T \\ X & -Q^{-1} & 0 \\ Y & 0 & -R^{-1} \end{bmatrix} < 0 \\ \begin{bmatrix} \gamma & X_0^T \\ X_0 & X \end{bmatrix} > 0 \\ X = X^T > 0 \end{cases} \tag{73}$$

If a solution exists, it is unique and the optimal control LQ is given by.

$$k_{LQ}^* = y^* x^{*-1} \tag{74}$$

The results using MATLAB are:

$$k_{LQ}^{*} = 1.0\mathrm{e}+05 \begin{bmatrix} -0.008953936493080 & 0.063988540619911 \\ -3.327576605308652 & -1.388793762344159 \end{bmatrix}$$

The related eigenvalues of the close loop plant are:

$$eig\ \ LQ = 1.0\mathrm{e}+05 \begin{bmatrix} -0.000093734812292 \\ -2.229694583033690 \end{bmatrix}$$

And the stability of the controller is verified.

Simulation

The zero regulation of the states (errors signals) is the main objective of the control design.

NOTE: in order to reduce the size of the report, only the moose test will be reported for the following controls.

Moose test

The Fig.37 shown the response of the system due to the LQ-controller and without controller for a disturbance related to moose test in the front steer angle.

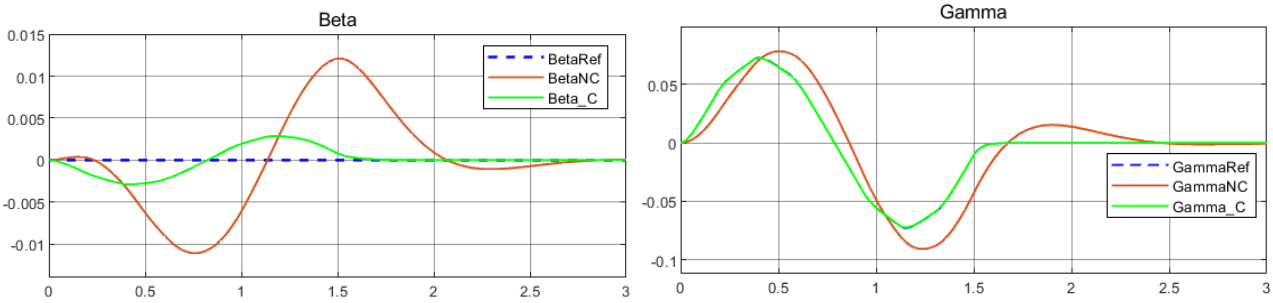

Fig.37 $\boldsymbol{\beta}$ Side slip angle of the vehicle body [rad] and $\boldsymbol{\gamma}$ Yaw rate of the vehicle body [rad/s]

it can be highlighted that the lateral slip angle $\boldsymbol{\beta}$ present a good behavior, while the yaw rate tends to follow the reference signal very close.

Fig.38 shows the corresponding errors regulated by the LQ-controller.

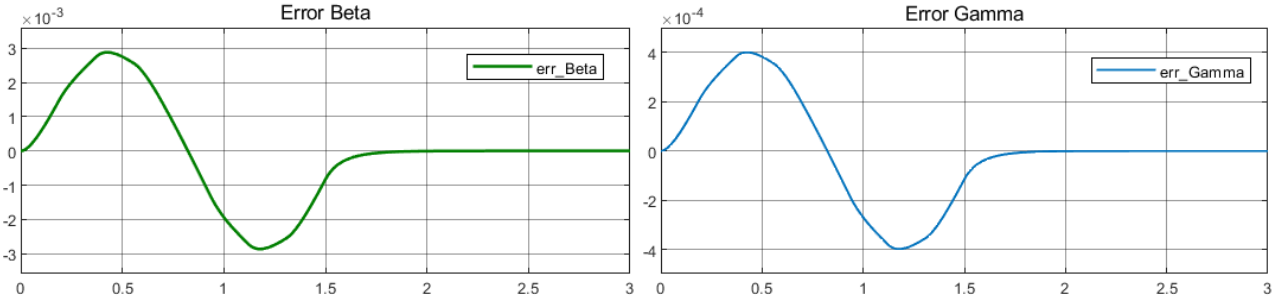

Fig.38 tracking errors of the states

The Fig.39 shown the input signals corresponding to Direct yaw moment and rear wheel steering angle generated by the LQ-controller.

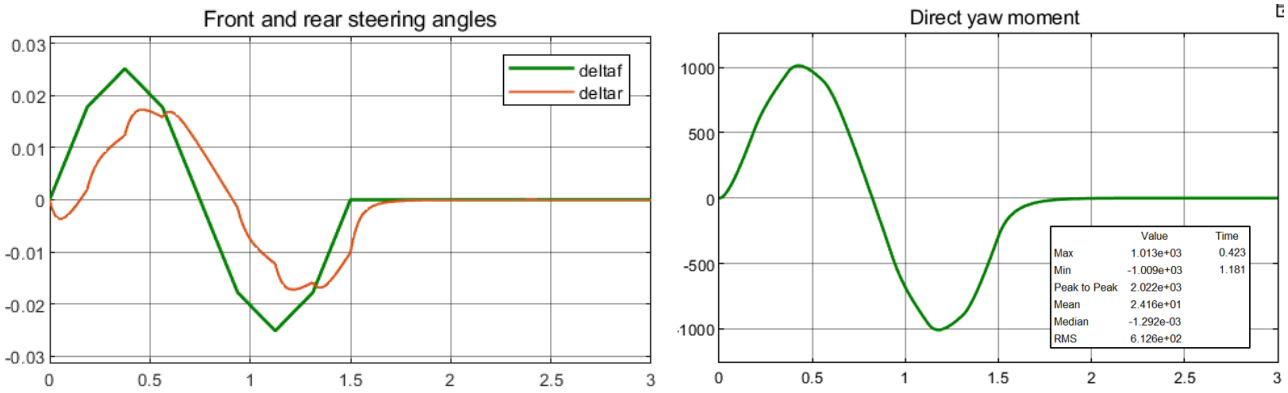

Fig.39 Rear wheel steering angle Direct yaw moment inputs

The first part shown the front and rear steering angle when the vehicle is moving at 80 km/h, the second part shown the Direct yaw moment due to the LQ-controller and it reaches a maximum value of 1013 and a minimum value of -1009 $[Nm]$.

Fig.40 refers to the system response taking into account the yaw rate as a function of the front wheel steering angle.

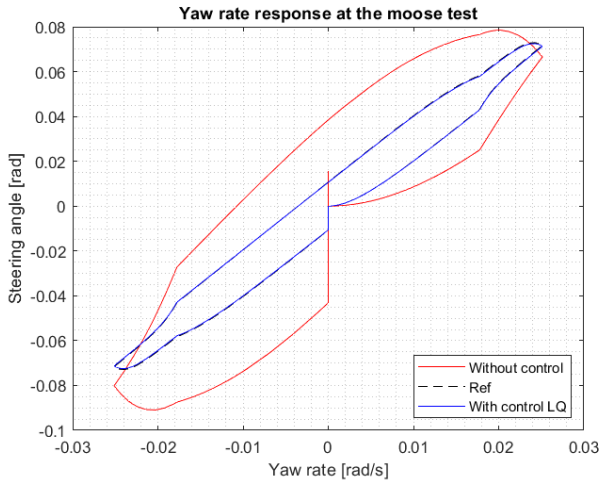

Fig.40 Yaw rate versus steering wheel angle

Looking at the results of the yaw rate versus the front steering wheel angle shown, it can be seen that the response becomes almost the same of the desired response when using the model matching controller with LQ-controller.

MULTIOBJECTIVE CONTROL

The previous LMI conditions that describe the optimization problems underlaying the synthesis of the various controllers are all convex in the variables X and Y. Then, they can be combined because the intersection of convex constrains is still a convex constrain.

5.5. H_2/H_∞ Optimal control

The objective of this multi-objective controller is made the closed loop $(A + Bk)$ asymptotically stable and minimize the norm H_2/H_∞. It seeks to find a balance between these two approaches. The goal is to design a controller that achieves good performance in terms of reference tracking and disturbance attenuation.

Given $a, b > 0$ fixed scalars the solution of this control is:

$$k^*_{H_2/H_\infty} = \min_{k \in S} a \|W\|_{H_\infty} + \|W\|_{H_2} \quad (75)$$

Formulation of this control in terms of LMI:

$$
\begin{gathered}
[x^*, y^*] = \min_{X,Y,Q} a\gamma_\infty + b\gamma_2 \\
s.t \\
\begin{bmatrix} AX + B_1Y + (AX + B_1Y)^T & B_2 & (C_1X + D_{12}Y)^T \\ B_2^T & -\gamma_\infty I & D_{11}^T \\ (C_1X + D_{12}Y) & D_{11} & -\gamma_\infty I \end{bmatrix} < 0 \\
\begin{bmatrix} AX + B_1Y + (AX + B_1Y)^T & B_2 \\ B_2^T & -I \end{bmatrix} < 0 \\
\begin{bmatrix} Q & (C_2X + D_{22}Y) \\ (C_2X + D_{22}Y)^T & X \end{bmatrix} > 0 \\
\gamma_2, \gamma_\infty > 0 \\
tr\{Q\} < \gamma_2 \\
X = X^T > 0
\end{gathered}
\tag{76}
$$

If a solution exists, it is unique and the optimal control H_2/H_∞ is given by.

$$
k^*_{H_2/H_\infty} = y^* x^{*-1} \tag{77}
$$

The results using MATLAB are:

$$
k^*_{H_\infty/H_2} = 1.0\text{e}+05 \begin{bmatrix} -1.476364740597886 & 4.302858804462907 \\ 0.312780553179327 & -0.910517744333006 \end{bmatrix}
$$

The related eigenvalues of the close loop plant are:

$$
eig\ H_\infty/H_2 = 1.0\text{e}+07 \begin{bmatrix} -0.000000248362388 \\ -1.515130563037480 \end{bmatrix}
$$

And the stability of the controller is verified.

Simulation

Moose test

The Fig.41 shown the response of the system due to the H_2/H_∞-controller and without controller for a disturbance related to moose test in the front steer angle.

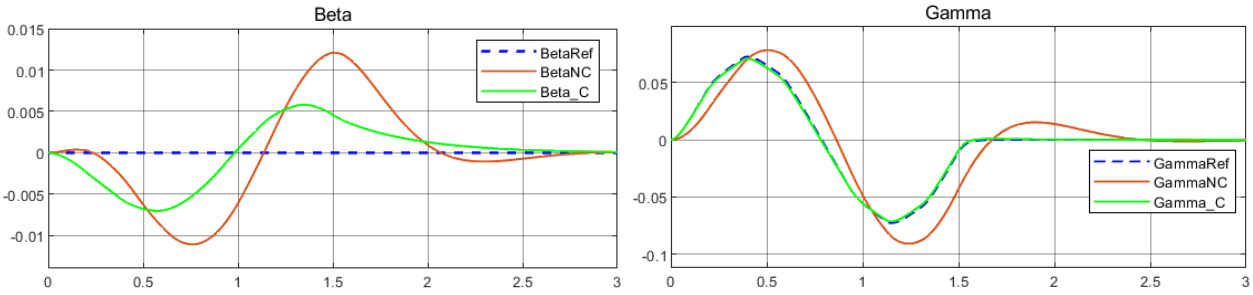

Fig.41 $\boldsymbol{\beta}$ Side slip angle of the vehicle body [rad] and $\boldsymbol{\gamma}$ Yaw rate of the vehicle body [rad/s]

it can be highlighted that the lateral slip angle $\boldsymbol{\beta}$ is more contained with respect to the uncontrolled one (BetaNC), while the yaw rate tends to follow the reference signal.

The Fig.42 shown the corresponding errors regulated by the H_∞/H_2-controller.

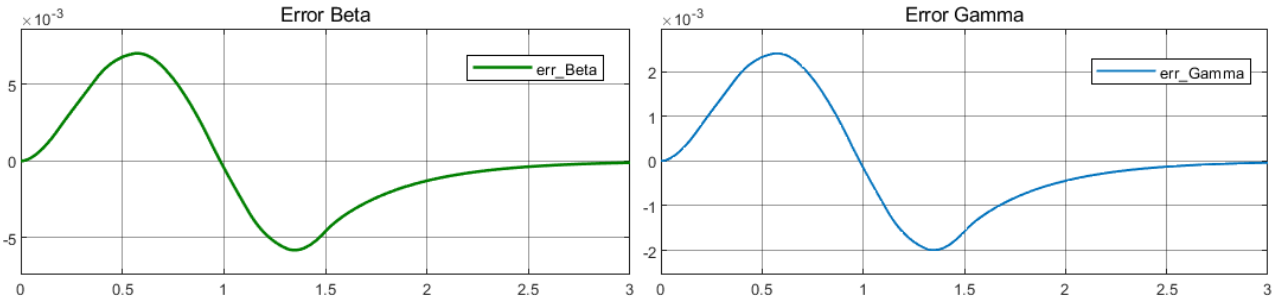

Fig.42 tracking errors of the states.

The Fig.43 shown the input signals corresponding to Direct yaw moment and rear wheel steering angle generated by the H_2/H_∞controller.

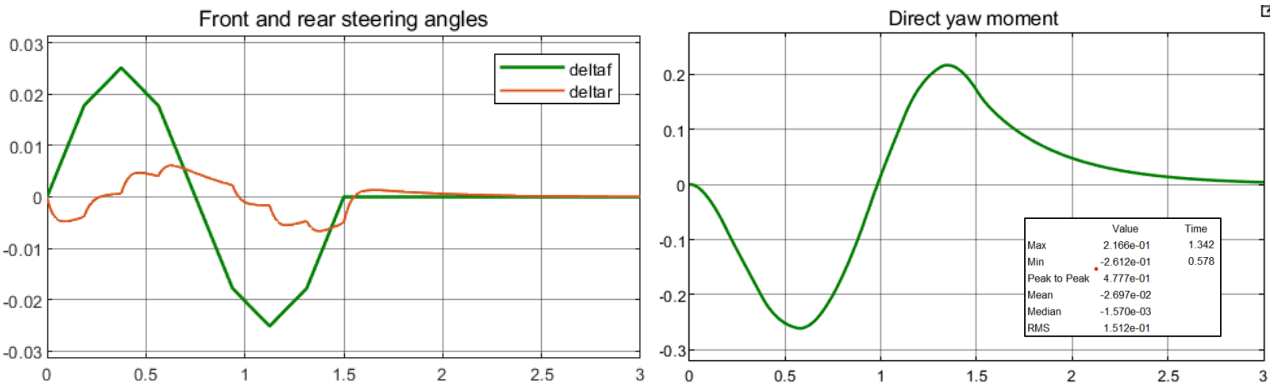

Fig.43 Rear wheel steering angle Direct yaw moment inputs

The first part shown the front and rear steering angle when the vehicle is moving at 80 km/h, the second part shown the Direct yaw moment due to the H_2/H_∞-controller and it reaches a maximum value of 0.2166 and a minimum value of -0.2612 [Nm].

Fig.44 refers to the system response taking into account the yaw rate as a function of the front wheel steering angle.

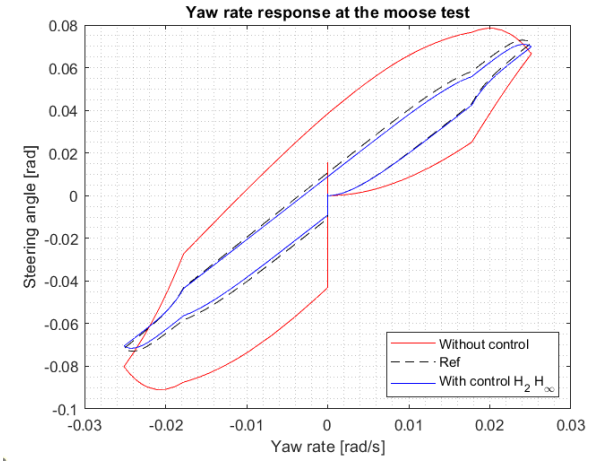

Fig.44 Yaw rate versus steering wheel angle

5.6. LQ- R stability optimal control

This implements a controller that allows to satisfy the zero regulation of the states and in the same time improve the evolution in the transient state of the Beta state (lateral slip angle). because in the LQ controller the evolution of gamma state presents a good performance, but beta has a grater error. Therefore, in this section the idea is improve the evolution of both states in the transient, placing the eigenvalues in an area determined by the parameters α , θ and r of the region $S(\alpha,r,\theta)$ refers to Fig.12.

The cost function of the LQ controller remain the same, however new constraints related to the LMI region $S(\alpha,r,\theta)$ are included, these constraints are described in the following LMI control problem.

$$
\begin{cases}
\min\limits_{X,Y} \gamma \\
s.v. \\
\begin{bmatrix} (AX+BY)+(AX+BY)^T & X & Y^T \\ X & -Q^{-1} & 0 \\ Y & 0 & -R^{-1} \end{bmatrix} < 0 \\
\begin{bmatrix} \gamma & X_0^T \\ X_0 & X \end{bmatrix} > 0 \\
X > 0 \\
[(AX+BY) + (AX+BY)^{\mathbf{T}} + \mathbf{2}\alpha X] < 0 \\
\begin{bmatrix} -rX & (AX+BY) \\ (AX+BY)^T & -rX \end{bmatrix} < 0 \\
\begin{bmatrix} \sin(\theta)((AX+BY) + (AX+BY)^{\mathbf{T}}) & \cos(\theta)((AX+BY) - (AX+BY)^{\mathbf{T}}) \\ \cos(\theta)(-(AX+BY) + (AX+BY)^{\mathbf{T}}) & \sin(\theta)((AX+BY) + (AX+BY)^{\mathbf{T}}) \end{bmatrix} < 0
\end{cases}
\tag{78}
$$

Where the selected parameters are

- α=250
- r=0
- θ=2e5

If a solution exists, it is unique and the optimal control $\mathrm{LQ-R}$ is given by.

$$
k^*_{\mathrm{LQ-R}} = y^* x^{*-1} \tag{79}
$$

The results using MATLAB are:

$$
k^*_{\mathrm{LQ-R}} = 1.0\mathrm{e}+07 \begin{bmatrix} -0.000150136962389 & 0.000012809144327 \\ 1.965616396590418 & -0.357739765064675 \end{bmatrix}
$$

The related eigenvalues of the close loop plant are:

$$
eig\ \mathrm{LQ-R} = 1.0\mathrm{e}+03 \begin{bmatrix} -0.250000244900939 \\ -8.313912079750979 \end{bmatrix}
$$

And the stability of the controller is verified.

Simulation

Moose test

The Fig.45 shown the response of the system due to the $\mathrm{LQ-R}$-controller and without controller for a disturbance related to moose test in the front steer angle.

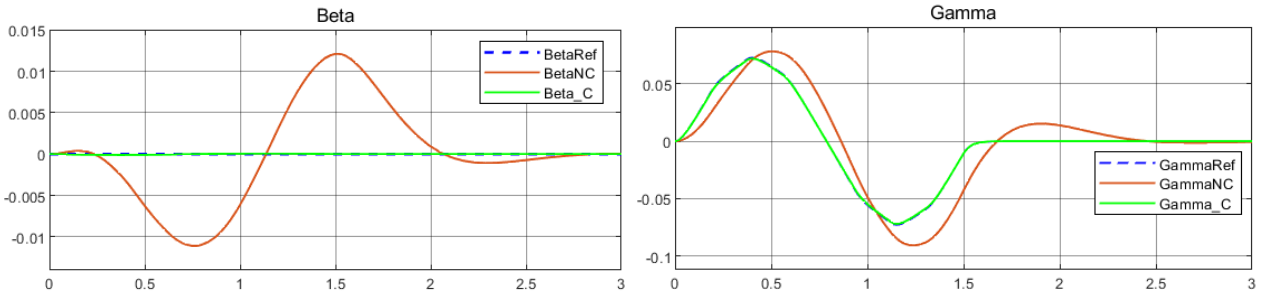

Fig.45 $\boldsymbol{\beta}$ Side slip angle of the vehicle body [rad] and $\boldsymbol{\gamma}$ Yaw rate of the vehicle body [rad/s]

it can be highlighted that the lateral slip angle $\boldsymbol{\beta}$ improve a lot with respect $\boldsymbol{\beta}$ only with LQ control, while the yaw rate continues following the reference with good performance.

The Fig.46 shown the corresponding errors regulated by the $\mathrm{LQ-R}$-controller.

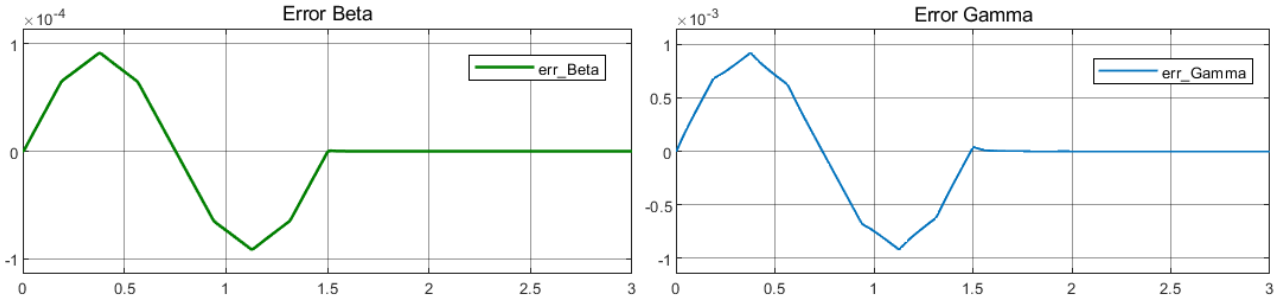

Fig.46 tracking errors of the states.

The Fig.47 shown the input signals corresponding to Direct yaw moment and rear wheel steering angle generated by the $\mathrm{LQ}-\mathrm{R}$ controller.

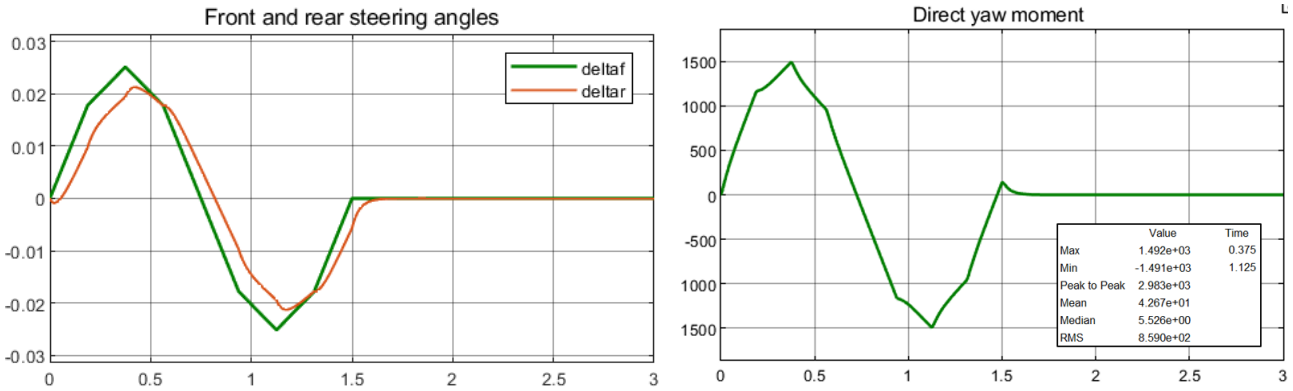

Fig.47 Rear wheel steering angle Direct yaw moment inputs

The first part shown the front and rear steering angle when the vehicle is moving at 80 km/h, the second part shown the Direct yaw moment due to the $\mathrm{LQ}-\mathrm{R}$ controller and it reaches a maximum value of 1492 and a minimum value of -1491 $[Nm]$.

Fig.48 refers to the system response taking into account the yaw rate as a function of the front wheel steering angle.

Fig.44 Yaw rate versus steering wheel angle

5.7. Comparison between the controllers

It is presented a comparation between the different controllers implemented in the previous section, in order to see which of them offers the best features. The comparation refers to the moose test performed for the controllers.

Regulation of the Beta state

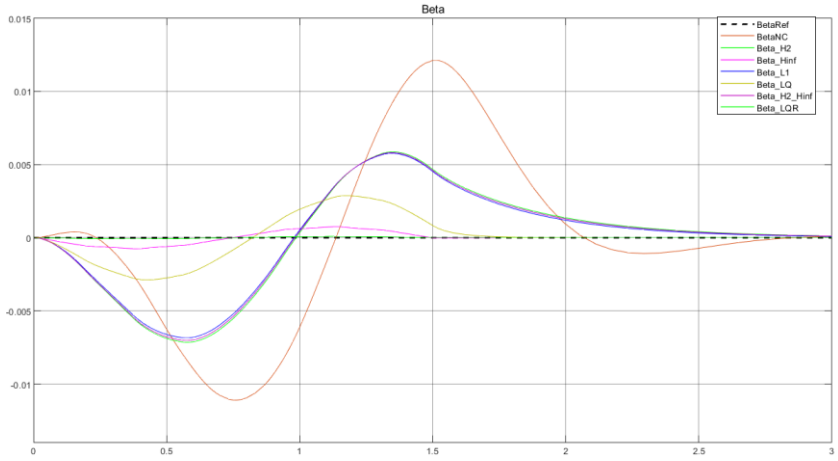

Fig.45 Comparation of the regulated Beta state

From Fig.45 can be seen that three controllers have better performance than the others: first the LQ-R controller has the best performance tracking the reference, second the H_inf controller that present also a good behavior and third the LQ controller. All the other controllers present almost the same behavior.

Regulation of the Gamma state

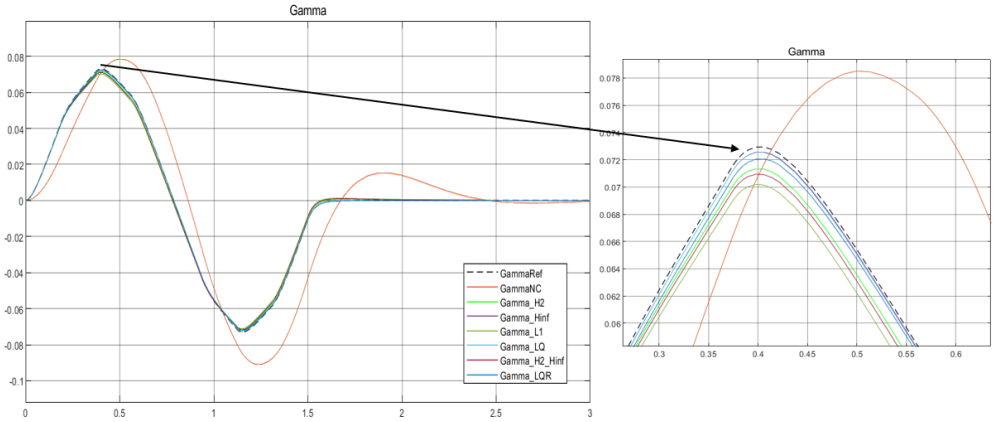

Fig.46 Comparation of the regulated Beta state

From Fig.46 can be seen that all controllers also present good behavior but the controllers H_inf, LQ have the best performance, in fact these two have the same performance.

Tracking error of the Beta state

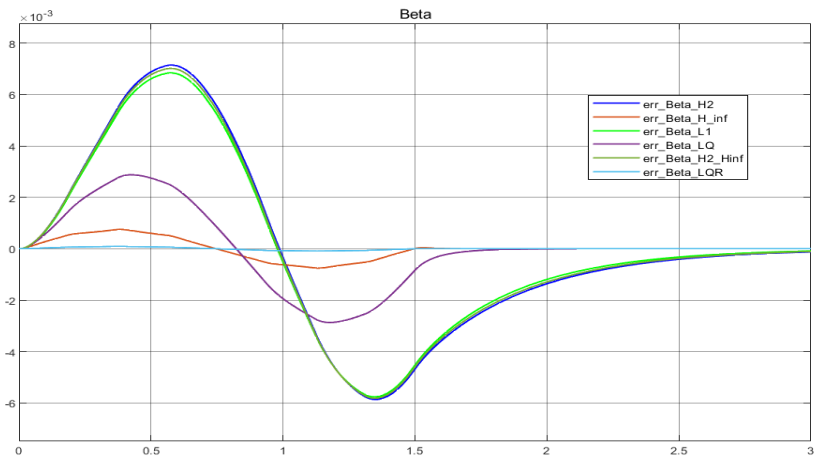

Fig.47 Comparation of the tracking error on Beta state

Fig.47 shows the errors corresponding to the beta state generated by the controllers.

Tracking error of the Gamma state

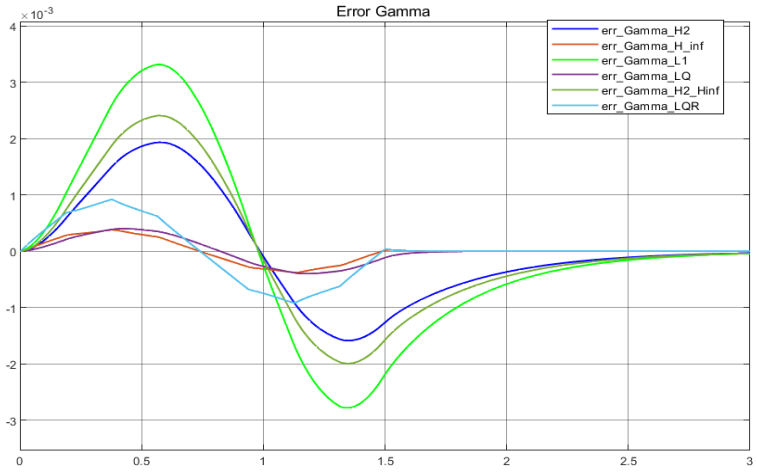

Fig.48 Comparation of the tracking error on Beta state

From Fig.48 can be seen more clearly that H_inf, LQ have the best performance.

Comparation of Direct yaw moment

Table.4 comparation of Direct Yaw Moment

Controllers	Direct yaw moment [Nm]	
	max	min
H2	0.008	-0.009
H_inf	1410	-1411
L1	27.94	-28.05
LQ	1013	-1009
H2/H_inf	0.2166	-0.2612
LQ-R	1492	-1491

Table 4 shows the Direct Yaw Moment output generated by the different controllers, the control H_inf and LQ-R are the controls that need more energy while H2 is the control that produces the lowest input.

According to the results shown, it can be highlighted that the LQ−R controller has the best behavior in the evolution of the side slip angle. However, it does not have the best behavior in the evolution of the Yaw Rate, it is also the controller that needs more energy in the Direct yaw moment. The same happens with the LQ controller, which presents good behavior in the evolution of the Yaw Rate but has more error in the evolution of the side slip angle in relation with LQ-R and H_inf controllers. However, the energy it needs for Direct Yaw moment is less in reference to the two controllers previously mentioned. The H_inf controller shows a good behavior in the side slip angle and in the Yaw rate in addition it needs less energy for the Direct Yaw moment in reference to the LQ-R controller.

5.8. Tracking problem with integral effect

In this section it is introduced an offset free effect in the control problem. Many tracking problems can be converted to classic regulation problems and solved as shown below:

Integral effect 1 pole – static state feedback

This control has one feedback gain and one feedforward gain as shown the Fig.49

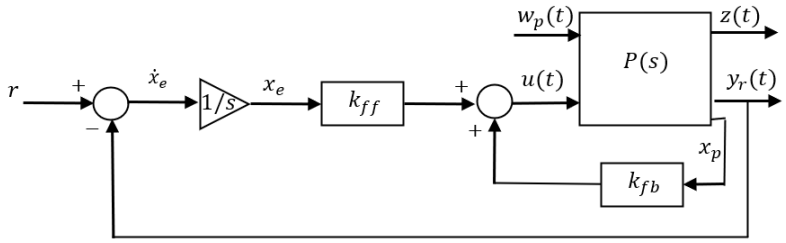

Fig.49 Integral effect 1 pole schematic

Where r is the reference signal, y_r is the reference output and w_p exogenous disturbance. The model in the state space is:

$$\begin{cases} \dot{x}_p(t) = A_p x_p(t) + B_u u(t) + B_w w_p(t) \\ z(t) = C_z x_p(t) + D_z u(t) + F_z w_p(t) \\ y_r(t) = C_r x_p(t) + D_r u(t) + F_r w_p(t) \end{cases} \quad (80)$$

In the scalar case, given a reference signal $r(t) = r$, the idea is regulating the error when the time tends to infinite.

$$\lim_{t\to\infty} e(t) = 0 \quad (81)$$

The error is given by $e(t) = r(t) - y_r(t)$. This problem can be converted in a regulation problem by introducing a new state component and finding a extended plant.

$$\dot{x_e}(t) = r(t) - y_r(t) = r(t) - C_r x_p(t) + D_r u(t) + F_r w_p(t) \quad (82)$$

The control action is:

$$u(t) = k_{ff} x_e(t) + k_{fb} x_p(t)$$

The Simulink schematic become:

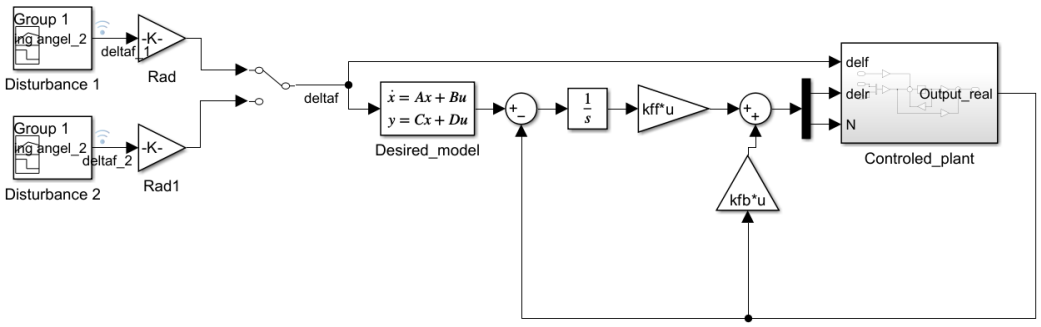

Fig.50 integral control 1 pole Simulink schematic

To check the behavior of the integral effect a new input for the front steering angle is generated and the reference signals are shown in Fig.51.

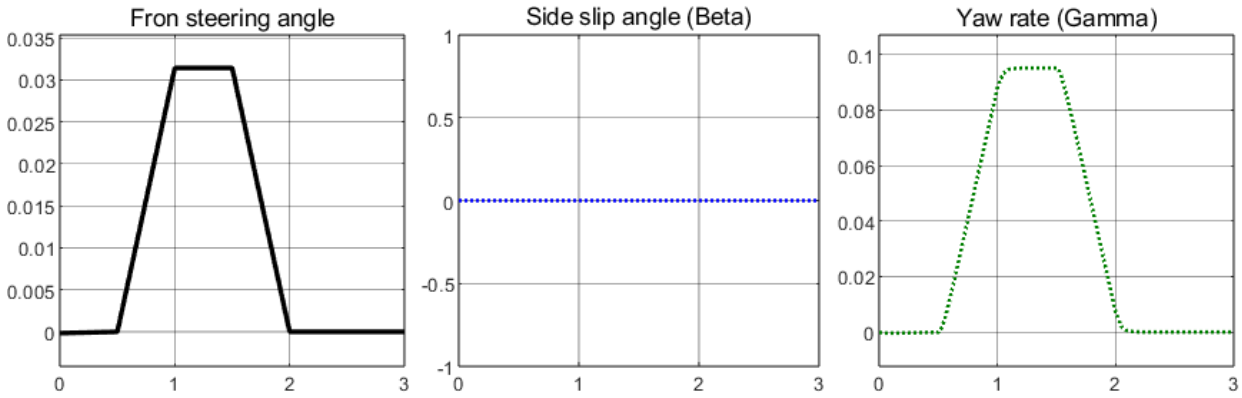

Fig.51 reference signals for the controls

Simulation

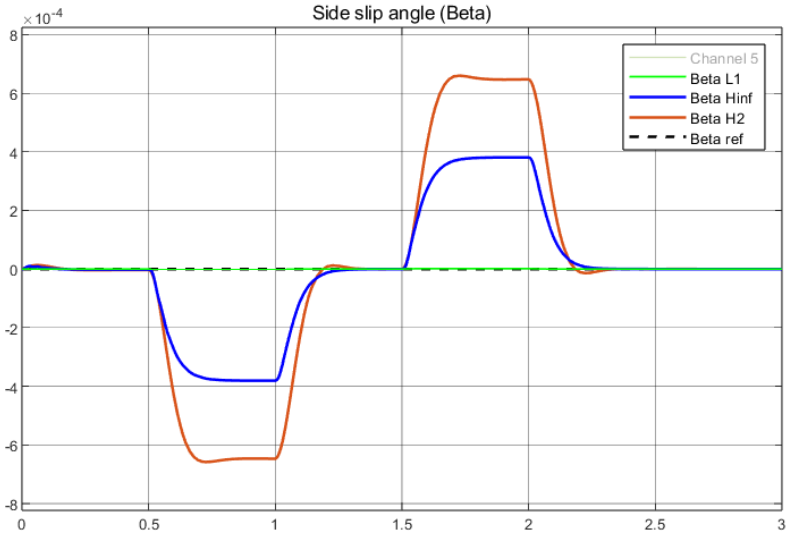

Fig.52 Side slip angle with integral control

From fig.52 is possible to see that the control L1 with integral control has the best performance.

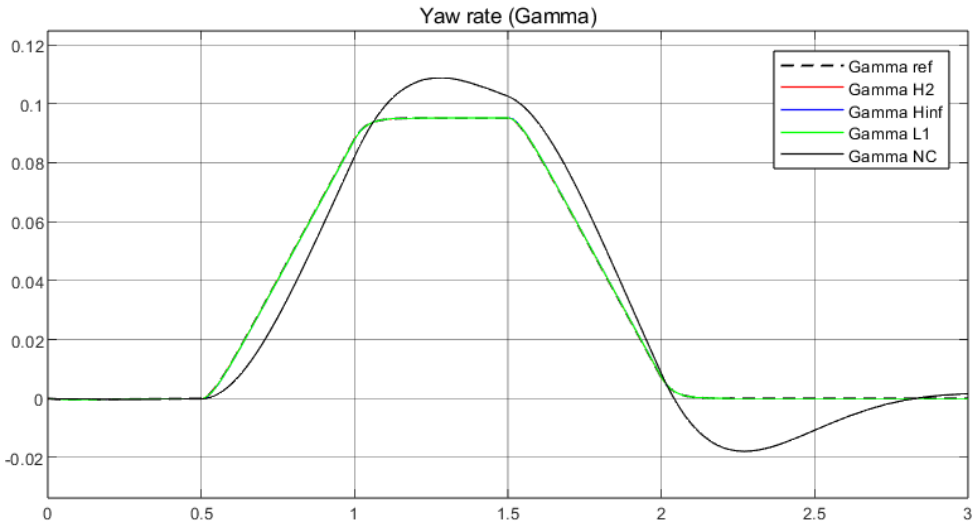

Fig.53 Yaw rate with integral control

Fig.53 shows the behavior of the controls for the Yaw rate using integral effect as we can se all has very good response.

Fig.54 refers to the tracking error of the yaw rate and the tracking error of the lateral slip angle.

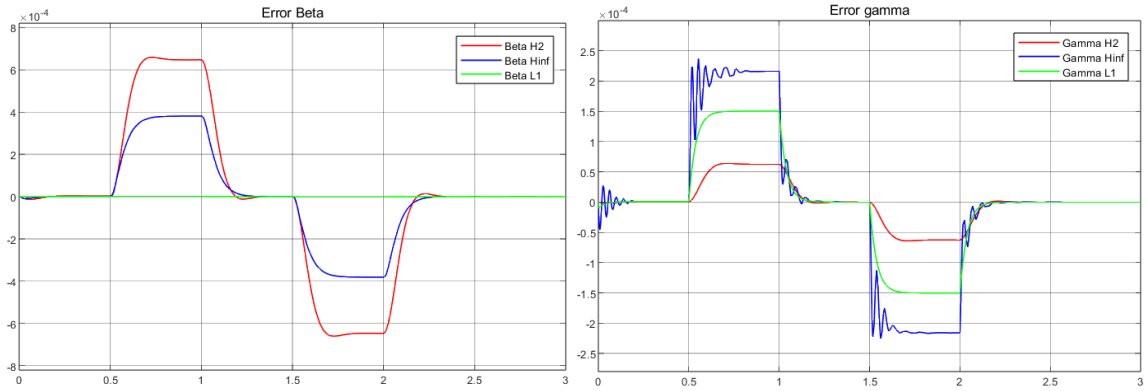

Fig.54 Side sleep angle and Yaw rate errors with control and integral control

According to Figures 52 and 54 it can be observed that controller $L1$ has better performance in lateral slip angle control while controller $H2$ has better performance in yaw rate control.

Table.5 comparation of Direct Yaw Moment

Controllers	Direct yaw moment [Nm]	
	max	min
H2	2124	-260.0
H_inf	2054	-190.9
L1	1967	-102.6

6. Robust Control

Given a model and a mathematical description of the model uncertainty the purpose is to design a control law able to ensure stability and/or performance for all values of allowed uncertainty. However, robust control has less performance with respect to optimal controls for LIT systems.

Until now the control has been designed for a constant speed of the vehicle. As it can be seen in Section 2, the system is strongly dependent on the speed of the vehicle, so the control that will be developed next has the purpose of controlling the vehicle at variable speeds.

The uncertainties are parametric because we know the state space representation of the system, but now the velocity is an uncertain parameter which varies from 50 to 100 km/h as example.

Define the state space uncertain representation.

It is used the Polytropic model to represent the uncertain system.

$$\dot{x}(t) = A(p)x(t) + B(p)u(t) + E(p)\delta_f(t)$$
$$y = Cx \qquad (83)$$

Where

$$p = \begin{bmatrix} p1 \\ \vdots \\ pn \end{bmatrix}, \qquad 0 \le pi \le 1, \quad \sum_{i=1}^{l} pi = 1 \qquad (84)$$

Because the analyzed problem only has one uncertain parameter the number of vertices is two. Then, the related matrices are:

$$A_1 = \begin{bmatrix} -\frac{C_f+C_r}{m*50} & -\frac{a_fC_f-a_rC_r}{m*50^2} - 1 \\ -\frac{a_fC_f-a_rC_r}{I_z} & -\frac{a_f{}^2C_f-a_r{}^2C_r}{I_zV} \end{bmatrix}, A_2 = \begin{bmatrix} -\frac{C_f+C_r}{m*100} & -\frac{a_fC_f-a_rC_r}{m*100^2} - 1 \\ -\frac{a_fC_f-a_rC_r}{I_z} & -\frac{a_f{}^2C_f-a_r{}^2C_r}{I_zV} \end{bmatrix}$$

$$B_1 = \begin{bmatrix} \frac{C_r}{m50} & 0 \\ -\frac{a_rC_r}{I_z} & \frac{1}{I_z} \end{bmatrix}, B_2 = \begin{bmatrix} -\frac{C_r}{m100} & 0 \\ -\frac{a_rC_r}{I_z} & \frac{1}{I_z} \end{bmatrix}, \; E_1 = \begin{bmatrix} \frac{C_f}{50V} \\ \frac{a_fC_f}{I_z} \end{bmatrix}, E_2 = \begin{bmatrix} \frac{C_f}{100V} \\ \frac{a_fC_f}{I_z} \end{bmatrix},$$

Due to the good performance of H_inf controller, it will be implemented in this section.

The optimal H_inf robust control is achieved if $\exists\, k \epsilon R^{mxn}$ such that $A(p)x(t) + B(p)u(t) + E(p)\delta_f(t)$ is asymptotically stable and $\|T_\infty\|_{H_\infty}^{wc} < \gamma \; if \; \exists\, x = x^T > 0, \exists\, Y \epsilon R^{mxn}$ and the following optimal problem has solution.

$$\begin{cases} [x^*, y^*] = \min_{X,Y,\gamma} \gamma \\ s.t \\ \begin{bmatrix} A_iX + B_{1,i}Y + (A_iX + B_{1,i}Y)^T & B_{2,i} & (C_{1,i}X + D_{12,i}Y)^T \\ B_{2,i}^T & -\gamma I & D_{11,i}^T \\ (C_{1,i}X + D_{12,i}Y) & D_{11,i} & -\gamma I \end{bmatrix} < 0 \\ i = 1 \dots l \\ \gamma > 0 \\ X = X^T > 0 \end{cases} \quad (85)$$

If a solution exists, it is unique and the robust optimal control H_∞ is given by.

$$k_\infty^* = y^* x^{*-1} \quad (86)$$

The results using MATLAB are:

$$k_\infty^* = 1.0\text{e}+08 \begin{bmatrix} -0.000004946790490 & -0.000003668018122 \\ -5.002891971684892 & -3.786194677577500 \end{bmatrix}$$

The related eigenvalues of the close loop plant are:

$$eig\ H_\infty = 1.0\text{e}+05 \begin{bmatrix} -0.000219997262022 \\ -1.321741888073772 \end{bmatrix}$$

And the stability of the controller is verified.

To check the performance of the robust control, a new disturbance signal was created in the Fig.55. It is possible to see that for each new velocity achieved a moos test is performed, in this way we can check the behavior of the robust control and notice if it works for all configurate velocities without loss the stability.

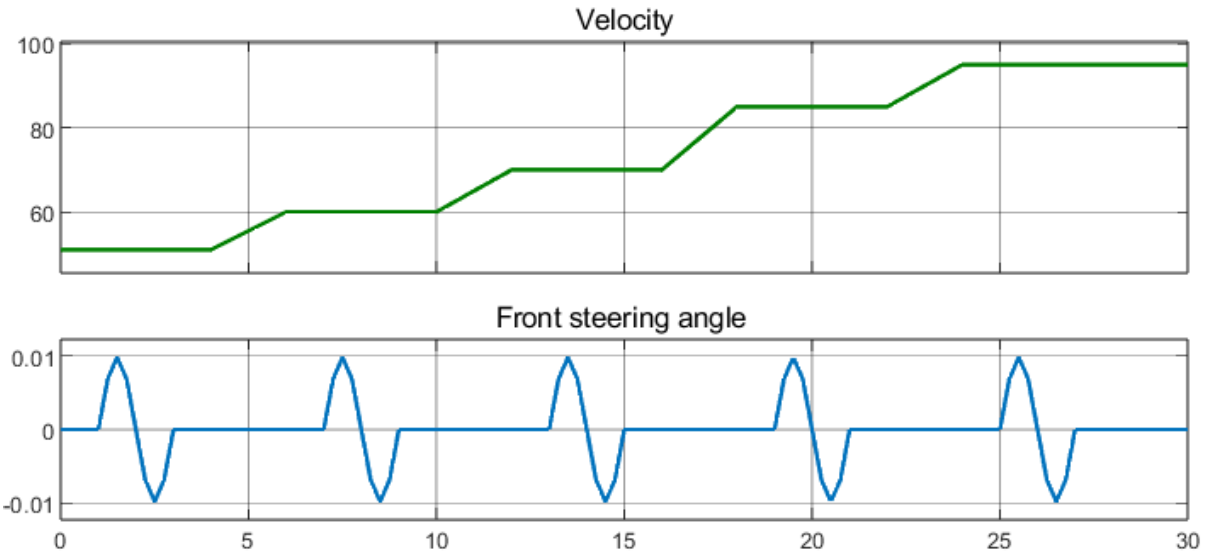

Fig.55 New input signals velocity and front steering angle

Simulations

The Fig.56 shown the response of the system due to the $robust\ H_\infty$-controller and without controller for a disturbance related to moose test in the front steer angle for different velocities.

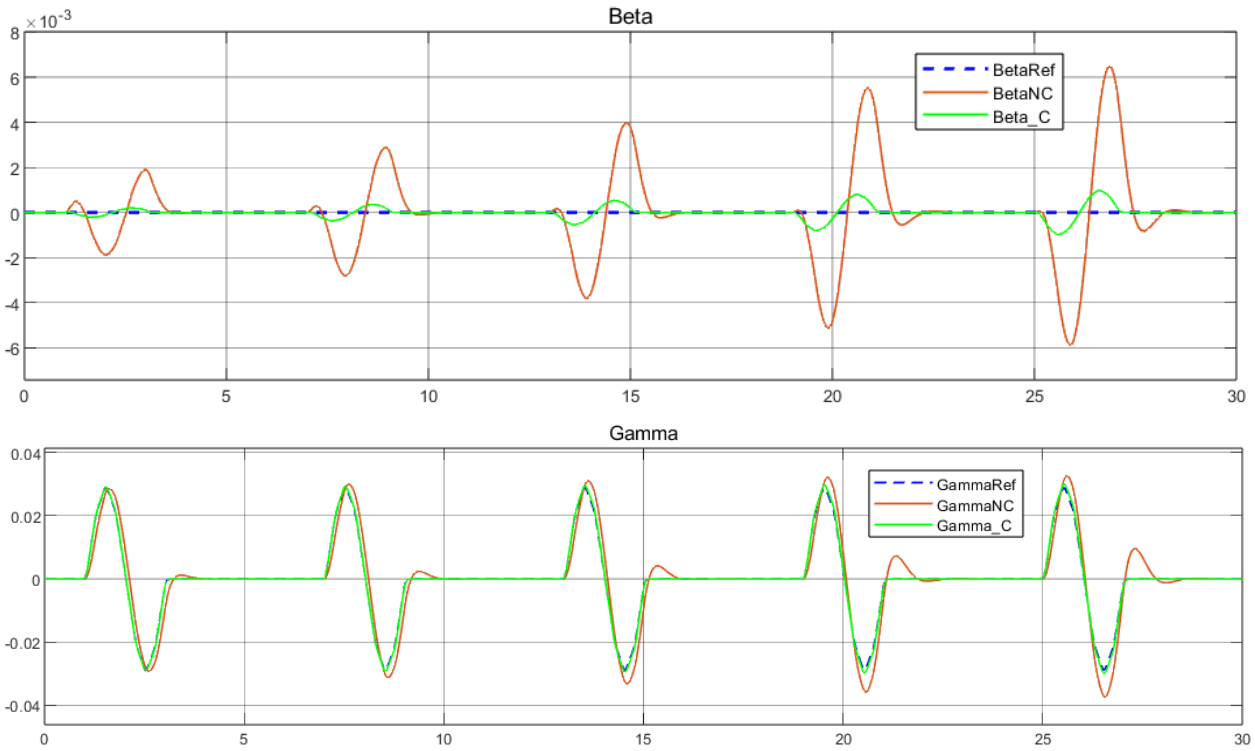

Fig.56 $\boldsymbol{\beta}$ Side slip angle of the vehicle body [rad] and $\boldsymbol{\gamma}$ Yaw rate of the vehicle body [rad/s]

it can be highlighted that the lateral slip angle $\boldsymbol{\beta}$ is much more contained with respect to the uncontrolled one (BetaNC) and the yaw rate tends to follow the reference signal almost perfectly for all velocities. Moreover, when the velocity increase the performance of the control start to get worse.

The Fig.57 shown the corresponding errors regulated by the H_∞-controller.

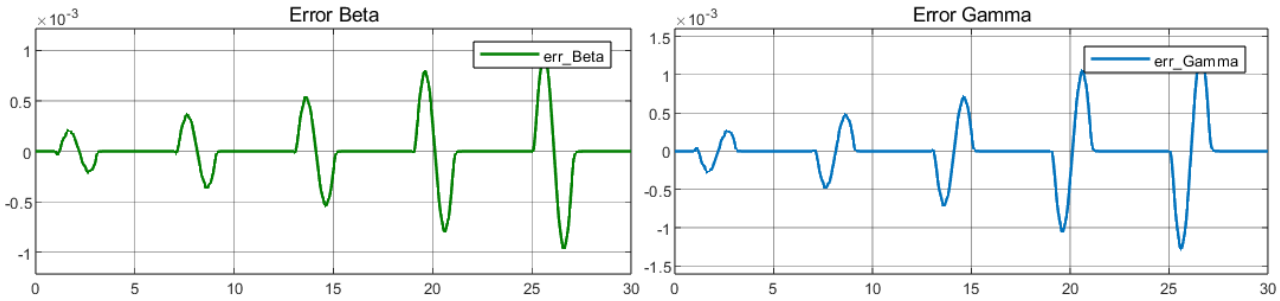

Fig.57 tracking errors of the states.

The Fig.58 shown the input signals corresponding to rear wheel steering angle and Direct yaw moment generated by the $robust\ H_\infty$-controller.

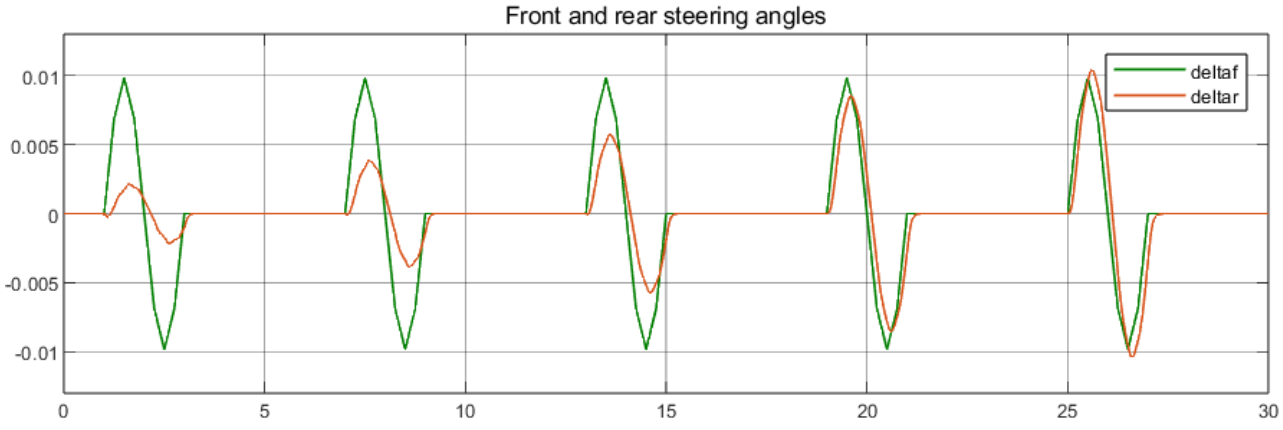

Fig.58 Rear wheel steering and angle Direct yaw moment inputs

The first part shown the front and rear steering angle when the vehicle is moving at different velocities, the second part shown the Direct yaw moment due to the $robust\ H_\infty$-controller and it reaches a maximum value of 752 and a minimum value of -752 [Nm] went the vehicle move at 95 km/h.

As we can see in the previous simulations the robust control work for all the velocities. Moreover, it does not have the best performance, in order to improve the control performance a new approach will be implemented in the next section.

6.1. LPV control

The Linear Parameter Varying version of the system is stated to give an uncertain modelling equal to the robust case, with the difference of hypotheses that we can measure the uncertain parameter online, which varies over time. Such information will be exploited in the synthesis by building a time-varying gain.

Therefore $p = p(t)$ consequently we will have $A(p(t))$ where:

$$\begin{aligned} \dot{x}(t) &= A(p(t))x(t) + B(p(t))u(t) + E(p(t))\delta_f(t) \\ y(t) &= C\big(p(t)\big)x(t) + D\big(p(t)\big)u(t) + D_w(p(t))\ \delta_f(t) \end{aligned} \tag{87}$$

It must be remembered that the value of the speed is determined through sensors in real time, which can measure the speed at any instant of time.

The matrices of the system depend on the ρn parameter through the following relationship.

$$\begin{aligned} A(\rho n) &= (1-\rho n)\underline{A} + \rho n\overline{A} \qquad B(\rho n) = (1-\rho n)\underline{B} + \rho n\overline{B} \\ E(\rho n) &= (1-\rho n)\underline{E} + \rho n\overline{E} \qquad D(\rho n) = (1-\rho n)\underline{D} + \rho n\overline{D} \\ D_w(\rho n) &= (1-\rho n)\underline{D_w} + \rho n\overline{D_w} \qquad C(\rho n) = (1-\rho n)\underline{C} + \rho n\overline{C} \\ \rho n &= \frac{v - v_{min}}{v_{max} - v_{min}} \end{aligned} \tag{88}$$

Then, the control gain will be obtained with the following equation.

$$k(\rho n) = (1-\rho n)\underline{k} + \rho n\overline{k} \tag{89}$$

Where the control gains $\underline{k}$, $\overline{k}$ are obtained front the matrices in the vertices v_{max}, v_{min}

With MATLAB's StateFlow the finite state machine has been implemented which allows to select the feedback control gain *k* based on the speed. This gain is computed according to H_∞-controller due to its good performance.

Fig.59 shows the StateFlow machine configuration implemented in the control. The control is the so-called Gain scheduling control.

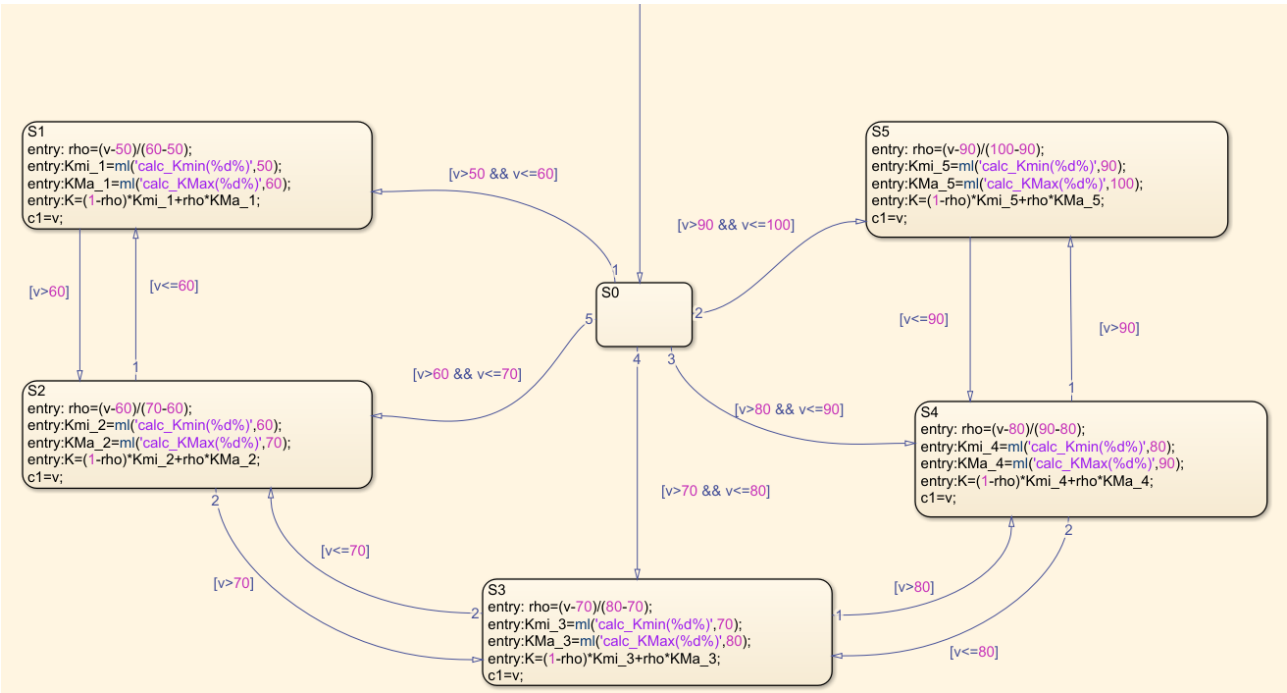

Fig.59 StateFlow machine configuration.

Considering the disturbance input and the velocity as in the case of robust control the responses of the LPV control are:

Simulations

Fig.60 shows the response of the system due to the $Gain\ Scheduling\ LPV\ H_\infty$-controller and without controller for a disturbance related to moose test in the front steer angle for different velocities.

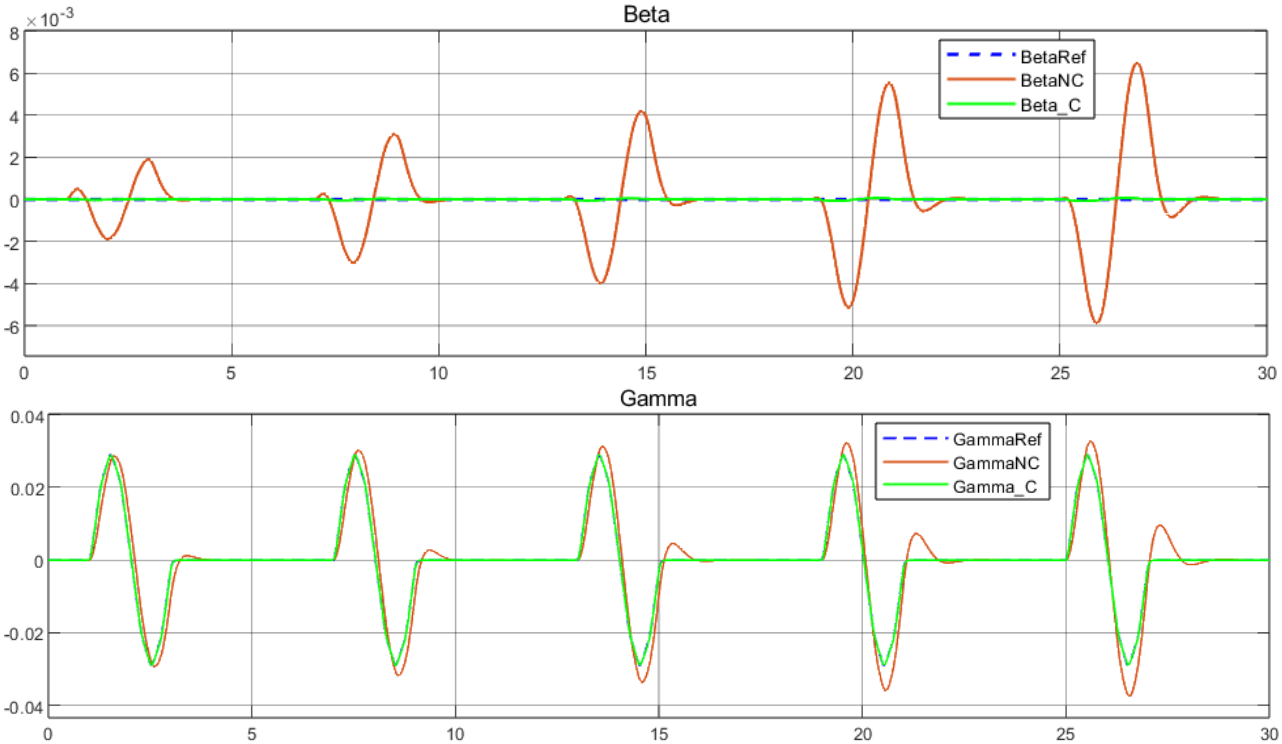

Fig.60 $\boldsymbol{\beta}$ Side slip angle of the vehicle body [rad] and $\boldsymbol{\gamma}$ Yaw rate of the vehicle body [rad/s]

it can be highlighted that the lateral slip angle $\boldsymbol{\beta}$ is much more contained with respect to the uncontrolled one (BetaNC) and the yaw rate tends to follow the reference signal almost perfectly for all velocities. Moreover, it is possible to see the performance of the control improve a lot with respect to robust control case.

The Fig.61 shown the corresponding errors regulated by the $Gain\ Scheduling\ LPV\ H_\infty$-controller.

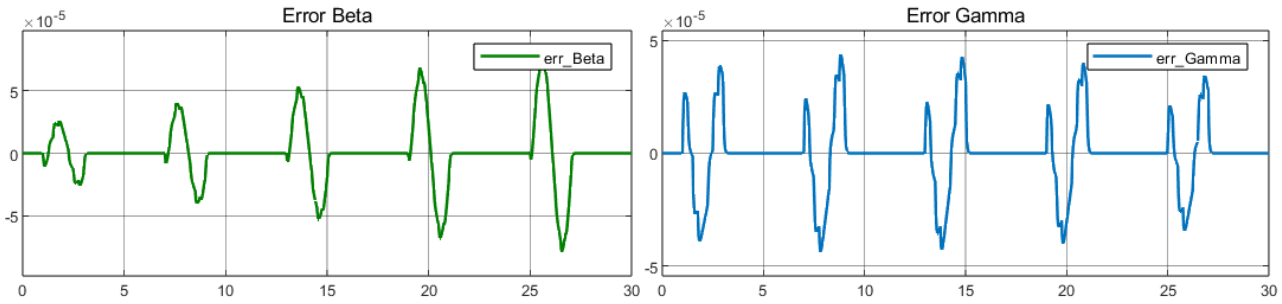

Fig.61 tracking errors of the states.

The Fig.62 shown the input signals corresponding to rear wheel steering angle and Direct yaw moment generated by the $Gain\ Scheduling\ LPV\ H_\infty$-controller.

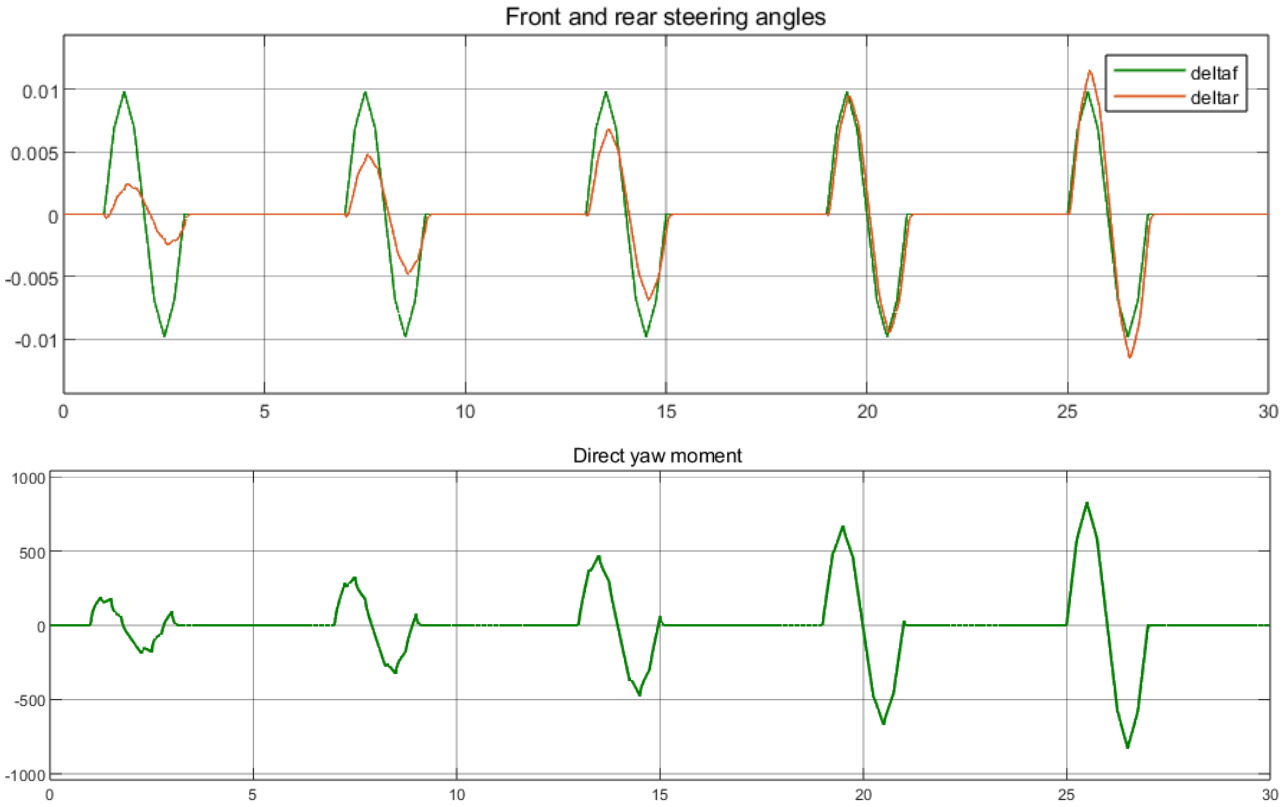

Fig.62 Rear wheel steering and angle Direct yaw moment inputs

The first part shown the front and rear steering angle when the vehicle is moving at different velocities, the second part shown the Direct yaw moment due to the $Gain\ Scheduling\ LPV\ H_\infty$-controller and it reaches a maximum value of 832 and a minimum value of -832 [Nm] went the vehicle move at 95 km/h.

As we can see in the previous simulations $Gain\ Scheduling\ LPV\ H_\infty$-controller work for all the velocities. Moreover, It is clearly noticeable that the behavior of the control has improved with respect to robust control.

7. Conclusions

Comparison between controls. From Fig.45 it can be seen that the three controllers have the best performance in the regularization of the beta state (Side slip angle). Firstly, the LQ-R controller has the best performance following the reference with a maximum error of 0.93e-04. Second, the H_inf controller also has good behavior with a maximum error of 7.31e-04. Finally, the LQ controller with a maximum error of 2.9e-03. All other drivers have higher errors and similar behavior. From Fig.46 it can be seen that all the controllers have good behavior regularizing the Gamma state (Yaw rate), but the H_inf and LQ controllers have the best performance with maximum errors of 3.9e-04 and 4.01e-04 respectively. However, due to the fact that the H_inf controller presents good behavior in the regularization of the two states, it is concluded that it is the one with the best performance.

The Model Matching Controller is a reference tracking problem by default, so by increasing an Offset Free effect with a pole and a Feedforward gain, the regularization of the states by the H_inf, H_2, and L1 controllers was vastly improved. However, the L1 controller has the best behavior in the regularization of the Beta state reducing the error to almost 0.

Finally, it can be observed that the robust control carried out with H_inf was capable of controlling the plant in the presence of an uncertain parameter (the velocity) however, it presents a poor performance. This was greatly improved by using an LPV plant design and considering that velocity is a parameter that we can measure online. Then, by applying a Gain Scheduling Controller was possible to generate a time-variant control gain that regulates the plant for each variation of velocity. In this way, the performance of the robust control was highly improved.

Bibliography

Casavola, A. (2022). class notes of the subject Vehicle Control. Rende: Universittà della Calabria, DIMES.

MASAO NAGAI , YUTAKA HIRANO & SACHIKO YAMANAKA (1997) Integrated Control of Active Rear Wheel Steering and Direct Yaw Moment Control, Vehicle System Dynamics, 27:5-6, 357-370, DOI: 10.1080/00423119708969336

https://www.sicurauto.it/news/sistemi-di-sicurezza/quattro-ruote-sterzanti-o-sterzo-attivo-sulle-ruote-posteriori/